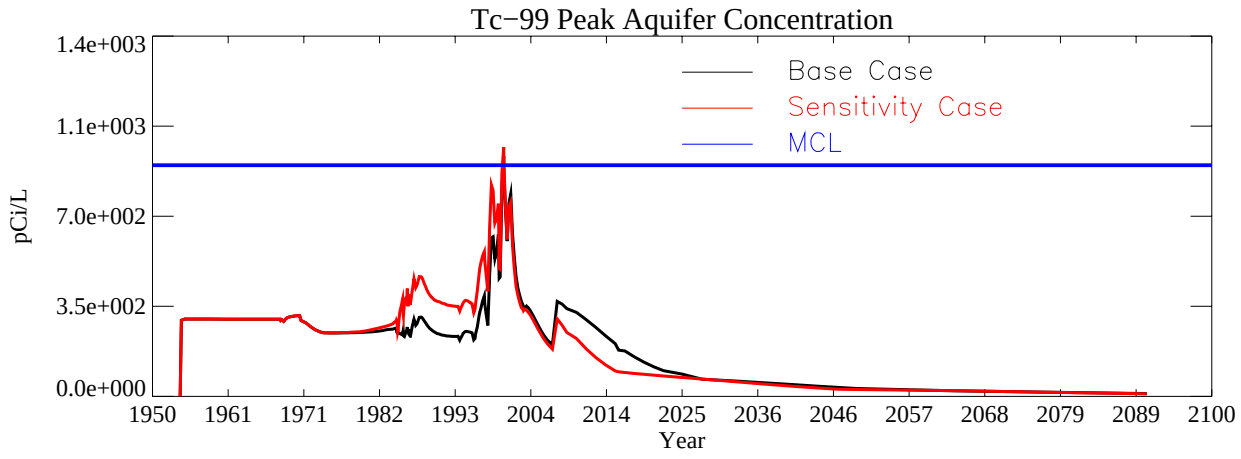

Figure A-10-30. Tc-99 peak aquifer concentration (pCi/L) for the 39-cm/year tank farm recharge rate case.

A-10.1.2.3 Tc-99 with Maximum Anthropogenic Recharge Rate

The peak simulated concentration in the vadose zone for this case was 3.34e+5 pCi/L in 1978 and occurs after the CPP-31 release date. The peak simulated concentration declined to 7.60e+3 pCi/L in 2005 and to 1.62e+3 pCi/L in 2095. Figures A-10-31 and A-10-32 present the vertical and lateral extent of the simulated vadose zone concentrations. The shallow vadose zone contamination located immediately northwest of the former percolation ponds is due to the CPP-22 OU 3-13 soil site (0.1 Ci), which was placed in the model in 1990.

Figure A-10-33 shows the peak vadose zone concentration through time. Peak vadose zone concentrations are much lower than the base case. The Tc-99 activity flux into the aquifer is illustrated in Figure A-10-34 and shows that the peak Tc-99 flux into the aquifer from the former percolation ponds and tank farm occurs much earlier than the base case. The Tc-99 concentration in key perched water wells is illustrated in Figure A-10-35.

Figure A-10-36 illustrates the horizontal aquifer concentrations, and the peak aquifer concentrations through time are given in Figure A-10-37. Peak aquifer concentrations resulting from the maximum recharge simulation are very similar to the base case, but less, and occurs earlier. The peak concentration in the year 2095 is 22 pCi/L, which is approximately two times the base case.

Figure A-10-31. Tc-99 horizontal vadose zone concentrations (pCi/L) for the maximum anthropogenic recharge rate case (MCL = thick red, MCL/10 = thin black, MCL*10 = thin red).

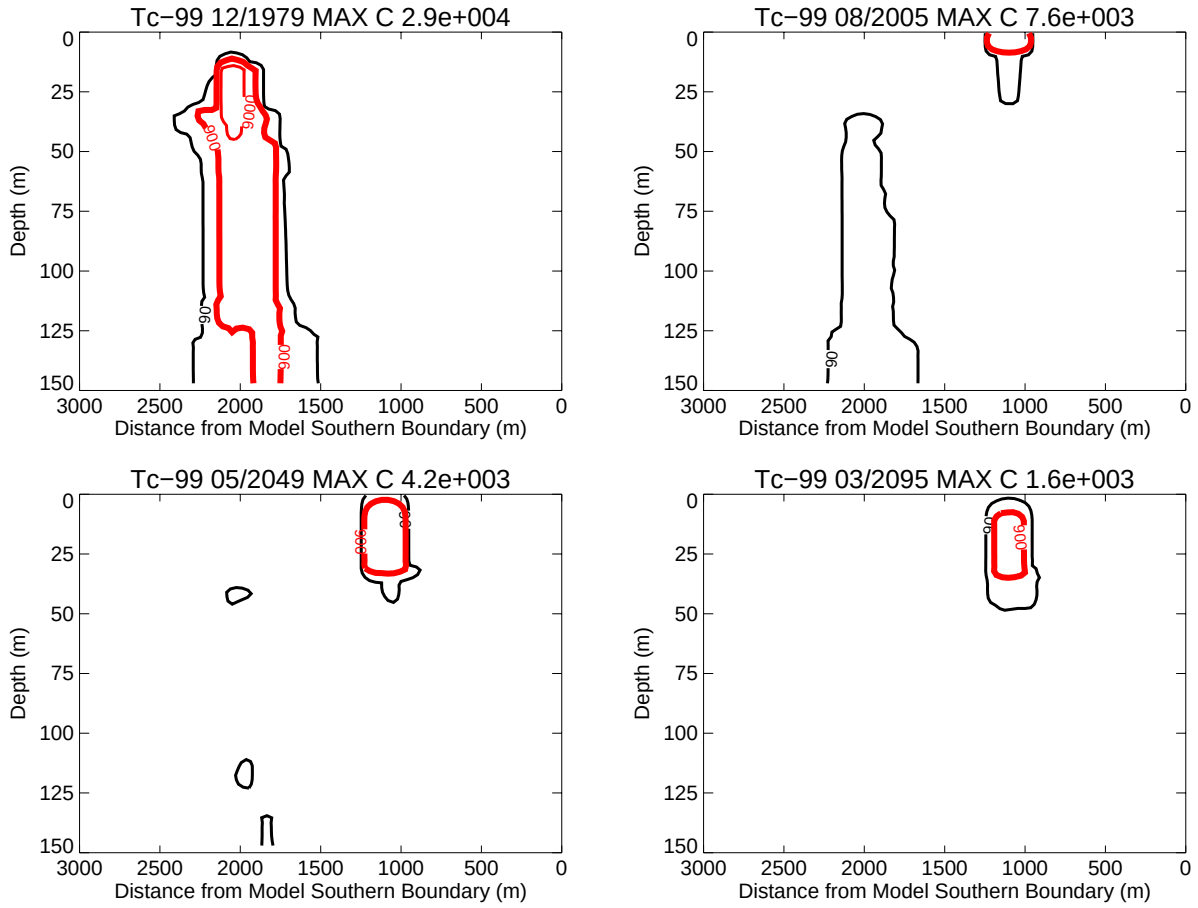

Figure A-10-32. Tc-99 vertical vadose zone concentrations (pCi/L) for the maximum anthropogenic recharge rate case (MCL = thick red, MCL/10 = thin black, MCL*10 = thin red).

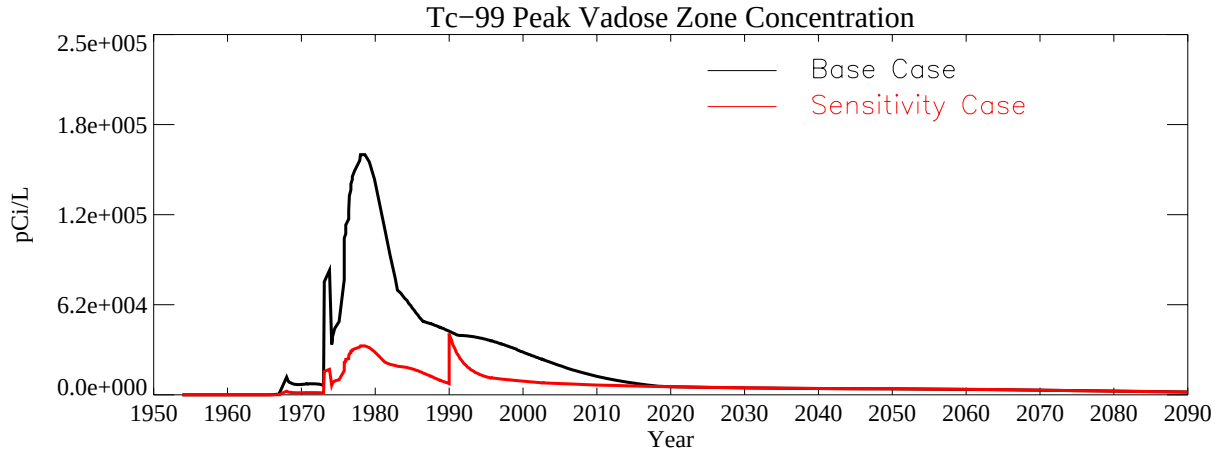

Figure A-10-33. Tc-99 peak vadose zone concentrations (excluding submodel area) (pCi/L) for the maximum anthropogenic recharge rate case.

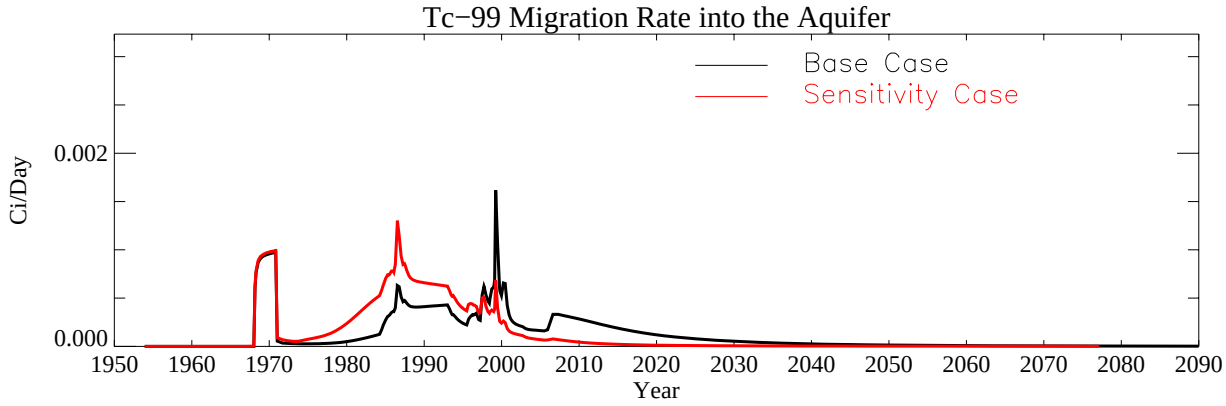

Figure A-10-34. Tc-99 flux into the aquifer (Ci/day) for maximum anthropogenic recharge rate case.

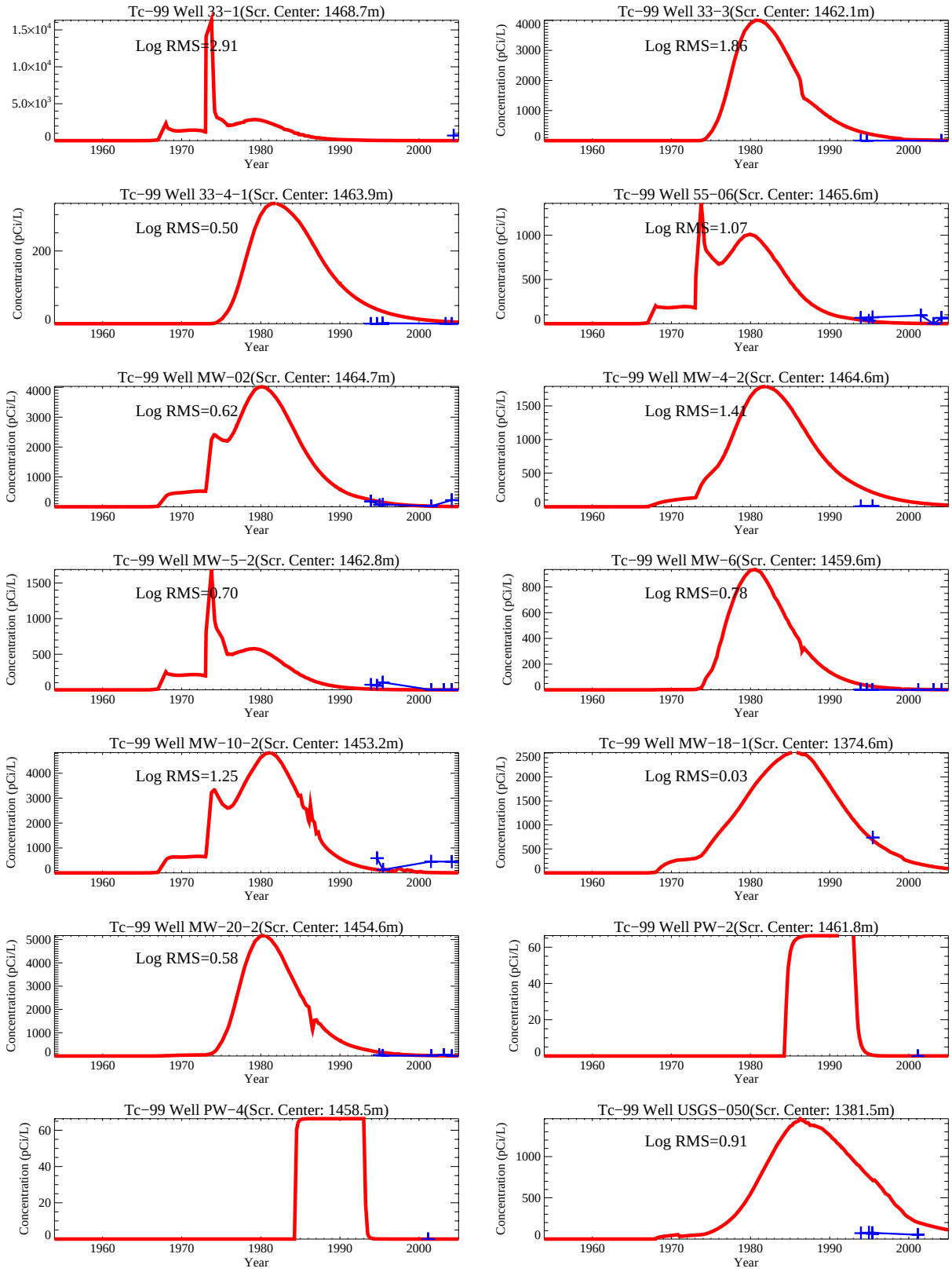

Figure A-10-35. Tc-99 concentration (pCi/L) in perched water wells for maximum anthropogenic recharge rate case (measured values = blue crosses, red = model at screen center).

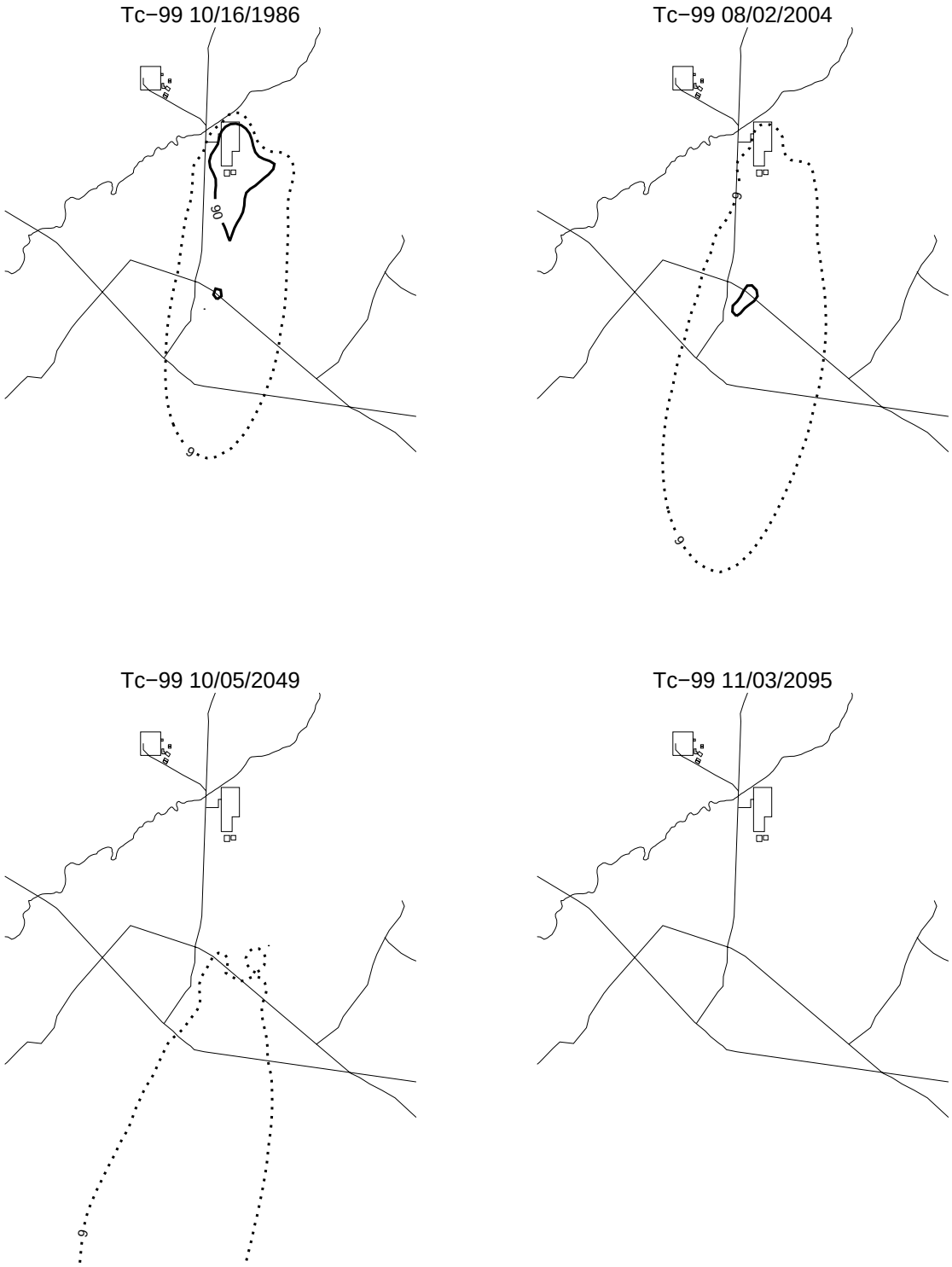

Figure A-10-36. Tc-99 aquifer concentrations (pCi/L) for the maximum anthropogenic rate case (MCL*10 = thin red, MCL = thick red, MCL/10 = thin black, MCL/100 = thin black dashed).

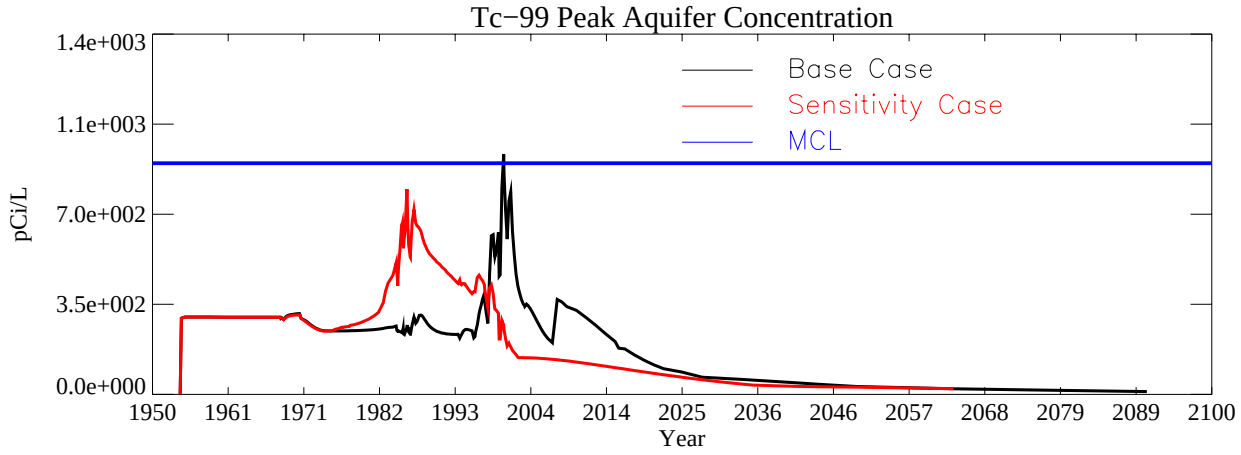

Figure A-10-37. Tc-99 peak aquifer concentration (pCi/L) for the maximum anthropogenic recharge rate case.

A-10.1.3 Tc-99 Preferential Flow Between the 380-ft Interbed and the ICPP-MON-A-230 Well

Routine sampling of the aquifer monitoring well ICPP-MON-230 2003 found Tc-99 concentrations at approximately twice the MCL. This was the first time that aquifer concentrations were found to exceed the MCL and prompted an investigation into the source of the Tc-99. The results of the Tc-99 investigation indicated that the source of the elevated Tc-99 in groundwater at well ICPP MON-A-230 was most likely attributable to historical liquid waste releases at the tank farm, in particular the Site CPP-31 release (ICP 2004).

The preponderance of evidence argues against the hypothesis that an improper annular seal at monitoring well ICPP-MON-A-230 could have allowed rapid downward migration of Tc-99 along the borehole to the aquifer. The 2005 Tc-99 results from new aquifer well ICPP-2021 (located 1500 feet away from MON-A-230) demonstrates that elevated Tc-99 concentrations are more widespread in the SRPA than previously believed. Moreover, the 2005 Tc-99 sampling results demonstrate that elevated Tc-99 concentrations are not present in the shallow perched water (TF-CH; 8.3 ±2.1 pCi/L) or deep perched water (TF-DP-L385; 7.8J ± 1.1 pCi/L) at the Tank Farm Well Set (DOE/ID, 2006). The low Tc-99 concentrations measured in the Tank Farm Well Set further bolsters the conclusion that the source of the elevated Tc-99 in the aquifer is not attributable to downward leakage of perched water at the boreholes of the Tank Farm Well Set. Rather, the most likely mechanism for transport of Tc-99 from contaminated tank farm soils to the aquifer is believed to be downward movement of contaminated water through the vadose zone to the water table, not short-circuiting down the borehole at well ICPP-MON-A-230.

The high aquifer concentrations of Tc-99 recently discovered in well ICPP-MON-A-230 could not be matched with the large-scale vadose zone model. The highest observed concentrations were approximately 3,000 pCi/L. The highest simulated concentrations were less than 1,000 pCi/L (see Section A-7.3.1). The high Tc-99 concentrations occurring in this well could be the result of a small-scale preferential flow path between the perched water near the 380-ft interbed beneath the tank farm and the aquifer near the ICPP-MON-A-230 well.

This hypothesis was investigated in the following manner: 1) the time history of the maximum Tc-99 concentration anywhere in the 380-ft interbed was used to define the preferential flow concentration, 2) a 10 gpm preferential pathway to the ICPP-MON-230 well location was placed in the aquifer model, and 3) the Tc-99 flux from the vadose zone into the aquifer model was uniformly reduced at all other blocks by the amount needed to maintain an unchanged total Tc-99 flux to the aquifer. This sensitivity simulation was only performed using the aquifer model and used the Tc-99 base case to define the Tc-99 flux.

The intent of this sensitivity simulation was to estimate the flow rate needed for a preferential flow path from the 380-ft interbed to the aquifer, which results in the observed concentrations at Well ICPP-MON-A-230. A ten gpm flow rate from the location of highest Tc-99 within the 380-ft interbed was needed. The total amount of Tc-99 transferred directly from the 380-ft interbed to the aquifer at the ICPP-MON-A-230 well location was 1.87 Ci, which is approximately 53% of the total Tc-99 (3.56 Ci) that was released to the tank farm. This flow rate resulted in a maximum aquifer concentration of 3,842 pCi/L in the year 1986.

This simulation indicates a relatively small preferential flow pathway could bring aquifer concentrations to that observed at ICPP-MON-A-230, but the area influenced was smaller than the current area observed to be over the MCL. The recently drilled ICPP-2020 and ICPP-2021 indicate this area may extend from north of the tank farm to possibly 1,000 ft southeast of the tank farm. The simulated arrival time for the very high concentration was much earlier than the current time and had fallen to 307 pCi/L by the year 2005. The peak aquifer concentration in the year 2095 was 9 pCi/L. The horizontal aquifer concentrations near INTEC for this simulation are given in Figure A-10-38, and the peak aquifer concentrations are shown in Figure A-10-39.

Figure A-10-38. Tc-99 aquifer concentrations (pCi/L) for the 10-gpm preferential flow path to well ICPP-MON-A-230 (MCL*10 = thin red, MCL = thick red, MCL/10 = thin black, MCL/100 = thin black dashed).

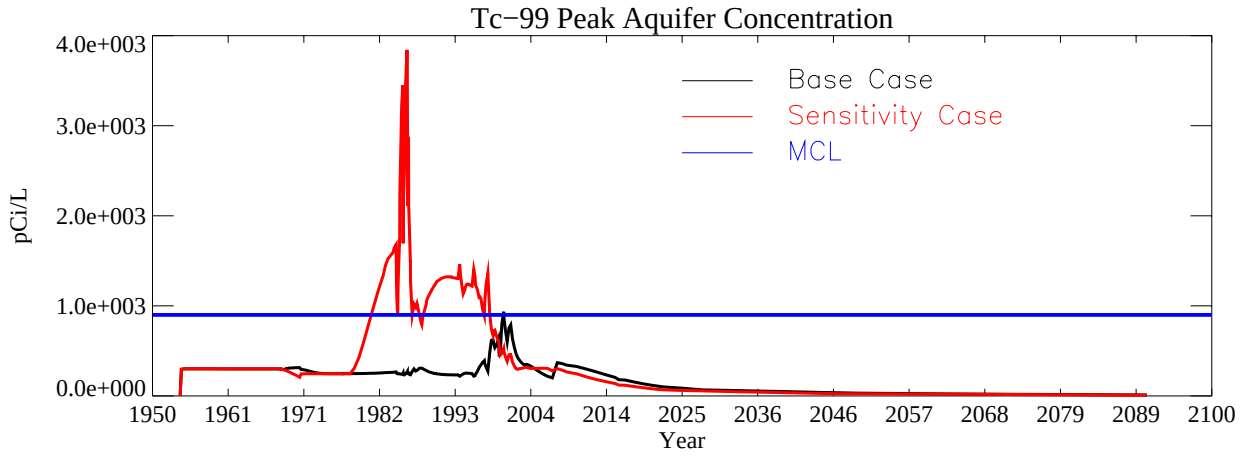

Figure A-10-39. Tc-99 peak aquifer concentration (pCi/L) for the 10-gpm preferential flow path to well ICPP-MON-A-230.

A-10.1.4 Tc-99 Service Waste Source Inventory

The Tc-99 concentrations were never monitored in the INTEC service waste. The service waste source term was estimated from the I-129 inventory and the ratio of Tc-99 to I-129 concentration measured in 2001 in the aquifer near the CFA (see Section A-9.2.3). As discussed in that section, I-129 and Tc-99 are very mobile and long-lived. If Tc-99 and I-129 are assumed to be transported identically from the CPP-3 injection well to the CFA monitoring wells, the ratio of measured values should be equal to the original disposal inventory. The aquifer wells north of the CFA were not used to obtain this estimate because the Tc-99 released in the tank farm may be influencing those ratios near INTEC.

The primary source of uncertainty is in how Tc-99 and I-129 are transported en route to the CFA. The sensitivity of the model to different Tc-99 service waste amounts was investigated by using the maximum concentration ratio found in the CFA wells. The maximum ratio was 25.1/1. This ratio resulted in a combined CPP-3 and percolation pond Tc-99 source of 37 Ci.

A-10.1.4.1 Maximum Service Waste Inventory for Tc-99

The peak simulated concentration in the vadose zone for this case was 1.64e+5 pCi/L in 1978 and coincides with the CPP-31 release date. The peak simulated concentration declined to 1.91e+4 pCi/L in 2005 and to 1.68e+3 pCi/L in 2095. Figures A-10-40 and A-10-41 illustrate the vertical and lateral extent of the simulated vadose zone concentrations.

Figure A-10-42 illustrates the peak vadose zone concentration through time. The peak vadose zone concentration is the result of the tank farm sources and increasing the service waste did not change these values. Therefore, both data appear as a single line on Figure A-10-42. The Tc-99 activity flux into the aquifer is illustrated in Figure A-10-43 and indicates that concentrations in the aquifer resulting from CPP-3 injection well failure and percolation ponds have nearly doubled. The Tc-99 concentration in key perched water wells is illustrated in Figure A-10-44. The shallow vadose zone contamination located immediately northwest of the former percolation ponds is due to the CPP-22 OU 3-13 soil site (0.1 Ci), which was placed in the model in 1990.

The increased Tc-99 service waste inventory had the most significant influence on the aquifer concentrations. Differences in the vadose zone model were only observable in a higher early activity concentration as a result of the CPP-3 injection well failure. The activity flux to the aquifer from the injection well failure increased from 0.001 Ci/day to 0.002 Ci/day.

Figure A-10-45 illustrates the horizontal aquifer concentrations, and peak aquifer concentrations through time are given in Figure A-10-46. The peak Tc-99 concentration in the year 2095 was 15 pCi/L, which is approximately 1.5 times the base case.

Figure A-10-40. Tc-99 horizontal vadose zone concentrations (pCi/L) for the maximum service waste inventory case (MCL = thick red, MCL/10 = thin black, MCL*10 = thin red).

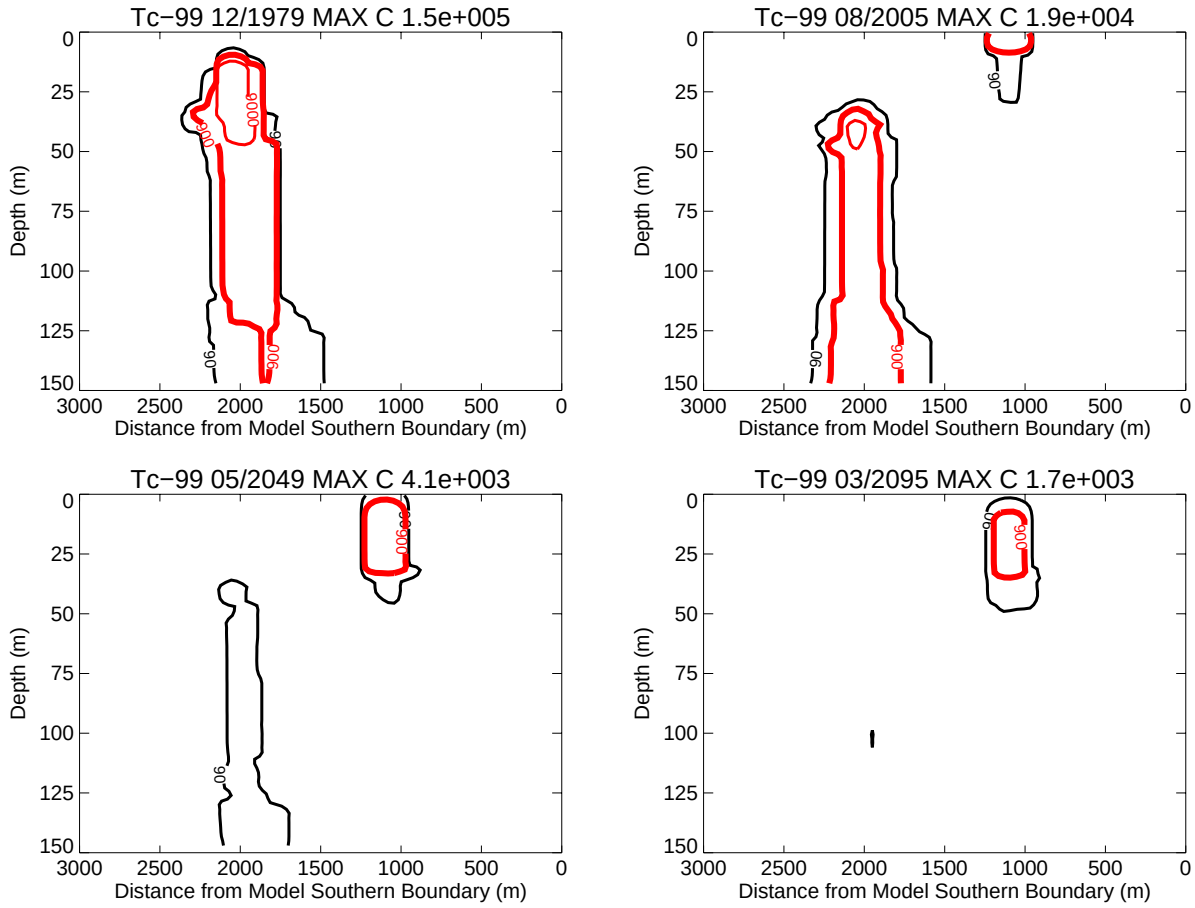

Figure A-10-41. Tc-99 vertical vadose zone concentrations (pCi/L) for the maximum service waste inventory case (MCL = thick red, MCL/10 = thin black, MCL*10 = thin red).

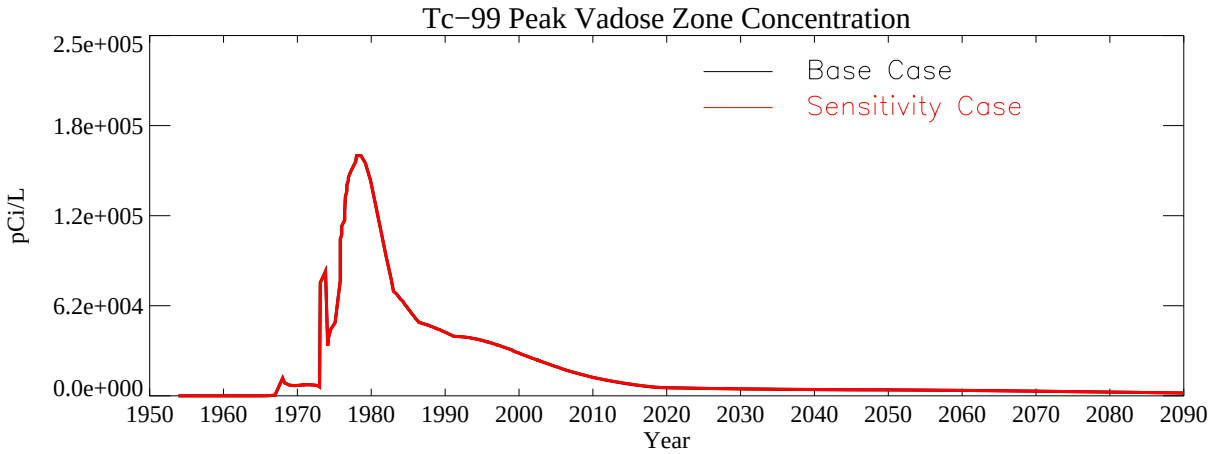

Figure A-10-42. Tc-99 peak vadose zone concentrations (excluding submodel area) (pCi/L) for the maximum service waste inventory case (sensitivity and base case data are identical).

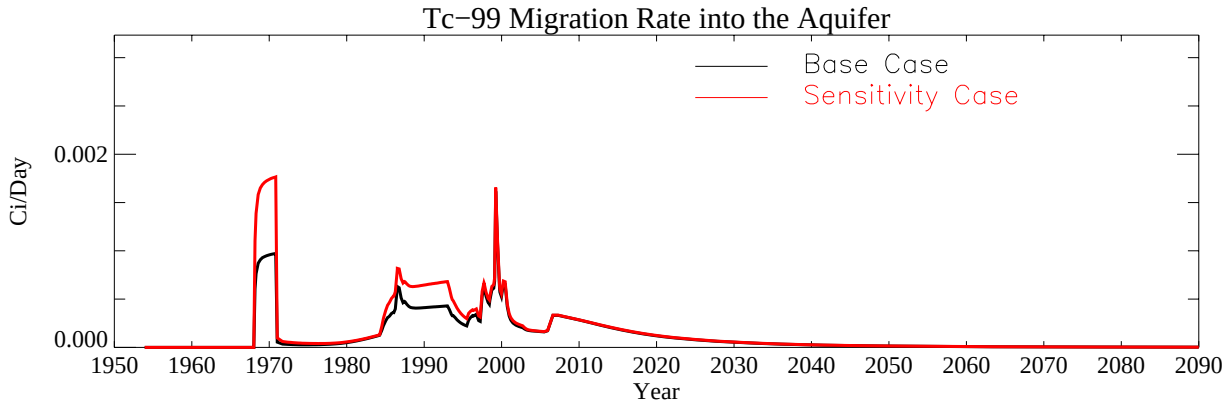

Figure A-10-43. Tc-99 flux into the aquifer (Ci/day) for the maximum service waste inventory case.

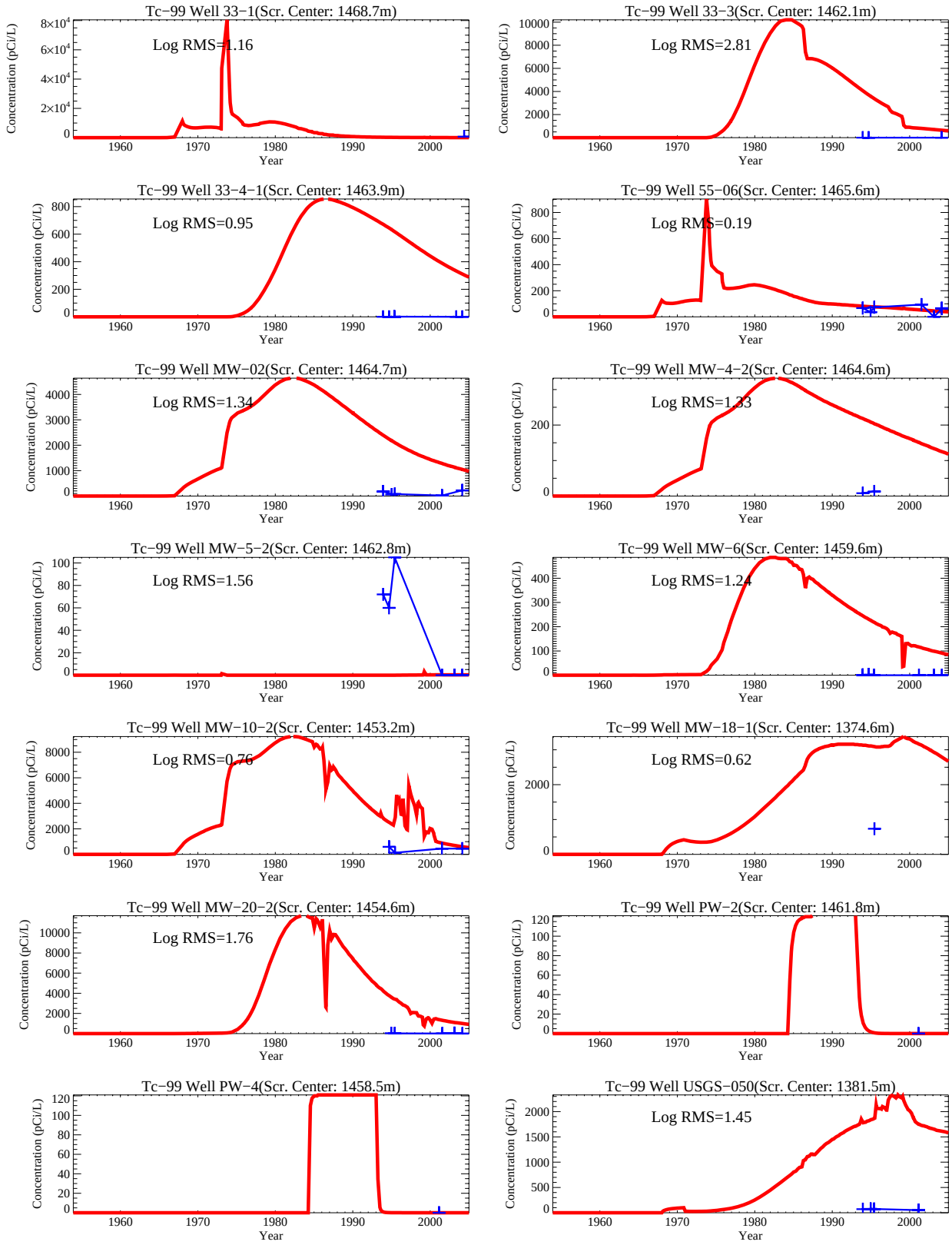

Figure A-10-44. Tc-99 concentration (pCi/L) in perched water wells for the maximum service waste inventory case. (measured values = blue crosses, red = model at screen center)

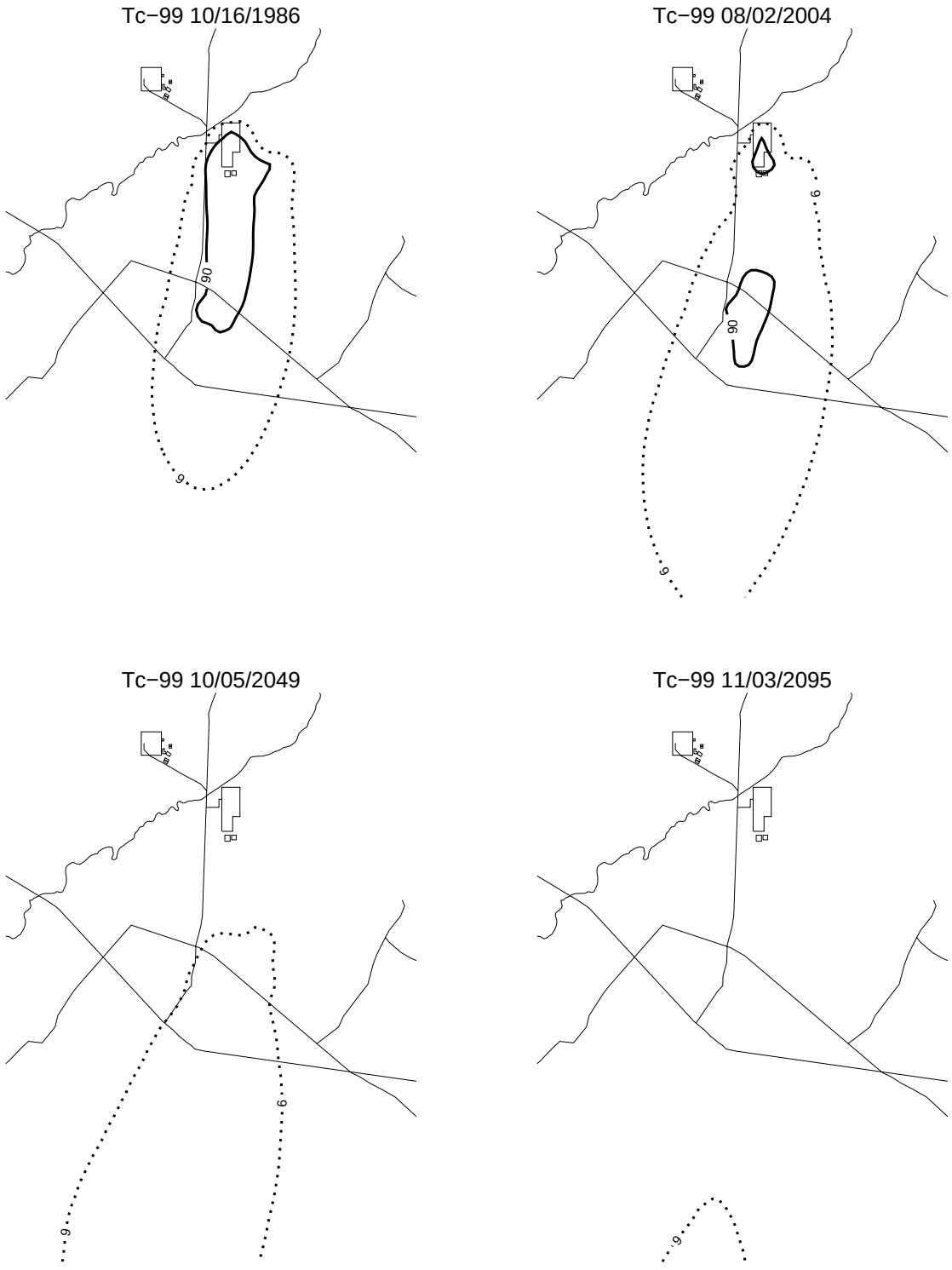

Figure A-10-45. Tc-99 concentrations (pCi/L) for the maximum service waste inventory case (MCL*10 = thin red, MCL = thick red, MCL/10 = thin black, MCL/100 = thin black dashed).

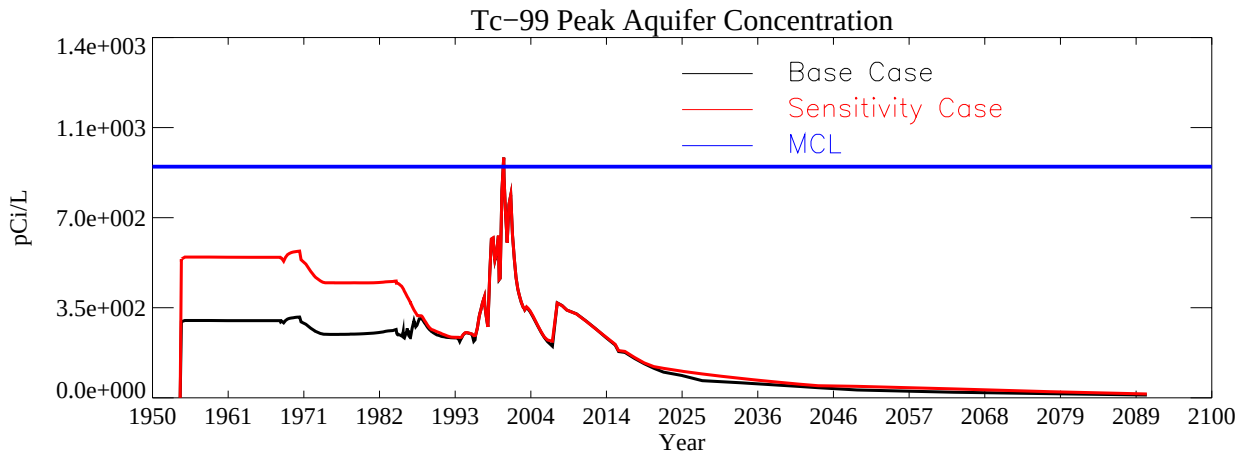

Figure A-10-46. Tc-99 peak aquifer concentration (pCi/L) for the maximum service waste inventory case.

A-10.1.5 Model Horizontal Grid Size

Contaminant concentrations and soil/rock saturations are functions of grid block discretization, primarily because of the implementation of the boundary conditions, where the incoming fluxes are assumed to be assigned to the node center. The incoming fluxes are partitioned within a given grid block (sorption), and phase velocities and pressures are calculated based on the pressure-saturation relationships within the grid blocks. Large grids can result in underpredicting contaminant concentrations and water saturations in addition to increasing numerical dispersion. Ideally, the model grid discretization should be determined by the minimum grid size required to obtain an invariant (size-to-size) result. However, limitations emplaced by computational resources typically dictate the minimum grid discretization. As a result of computational limitations, discretization is often a trade-off between larger block sizes, smaller simulation domains, and longer run times. Small simulation domains may have boundaries that influence the solution. For example, a lateral boundary could restrict lateral water movement and create deeper perched water, which would not occur in the larger domain, while more grid blocks of the same size necessary to represent the larger flow domain require excessive run times. The OU 3-14 model discretization was guided by the need to capture the very large Big Lost River and percolation pond recharge sources and the need to have a computationaly tractable model.

The model sensitivity to the horizontal grid discretization was assessed by simulating a subdomain of the northern INTEC using the same model parameters and a smaller horizontal grid block size. The OU 3-14 used a 100- x 100-m horizontal grid and the subdomain model used a 50- x 50-m horizontal grid. The submodel includes a smaller reach of the Big Lost River, which also may contribute to differences between the subdomain model and the base model. The submodel domain is illustrated in Figure A-10-47.

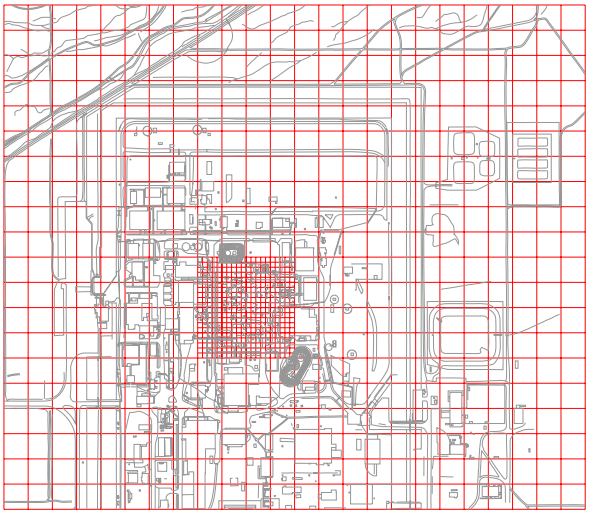

Figure A-10-47. Subdomain model horizontal discretization.

A-10.1.5.1 Tc-99 Horizontal Discretization Sensitivity Results

The peak simulated concentration in the vadose zone for this case was 6.42e+5 pCi/L in 1978 and occurs after the CPP-31 release date. The peak simulated concentration declined to 7.4e+4 pCi/L in 2005 and to 3.64e+3 pCi/L in 2095. Figures A-10-48 and A-10-49 illustrate the vertical and lateral extent of the simulated vadose zone concentrations.

Figure A-10-50 gives the peak vadose zone concentration through time. The peak concentration resulting from the CPP-31 release increased by a factor of 3.9 simply as a result of decreasing the grid size. The Tc-99 activity flux into the aquifer is illustrated in Figure A-10-51 and does not contain the service waste pond peak fluxes that occurred in the base case during the 1980s and 1990s because the submodel domain did not include the ponds. The Tc-99 concentration in key perched water wells is illustrated in Figure A-10-52.

The amount of horizontal spreading in this submodel is less than that predicted by the base case. As a result, the submodel overpredicted concentrations in the tank farm hot spot located south and east of the tank farm (i.e., CPP-33-1 and MW-10-2) but underpredicted concentrations further from the tank farm (i.e., wells MW-5-2 and MW-55-06). The submodel would require a higher dispersivity to match the far and near wells. This would result in lower peak concentrations and better agreement between the submodel and base case model. In general, the behavior of the submodel Tc-99 and the base case Tc-99 is similar. The tank farm contaminants move south and east of the tank farm in the upper shallow perched water. Both models predict the Big Lost River to have a large impact on Tc-99 flux into the aquifer. In both cases, the peak aquifer flux immediately follows the minimum peak flow year for the Big Lost River recorded at Lincoln Boulevard bridge gauge in 1999.

Aquifer concentrations for these simulations are given in Figure A-10-53, and Figure A-10-54 illustrates peak aquifer concentrations through time. The peak aquifer concentration was 783 pCi/L in 1970 and 192 pCi/L in 2005, which were very near the base case values. The peak aquifer concentration in the year 2095 was 14 pCi/L, which was slightly higher than the base case value.

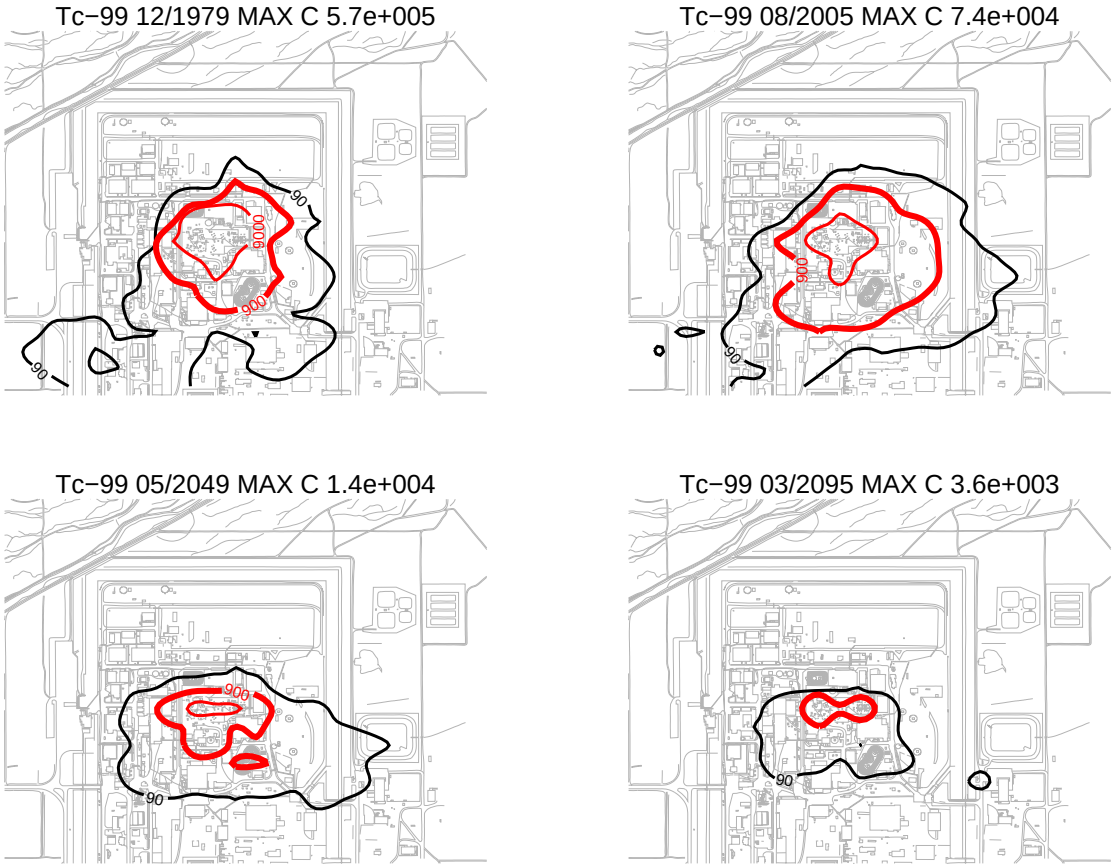

Figure A-10-48. Tc-99 horizontal vadose zone concentrations (pCi/L) for the 50- x 50-m submodel case (MCL = thick red, MCL/10 = dotted, MCL*10 = thin red).

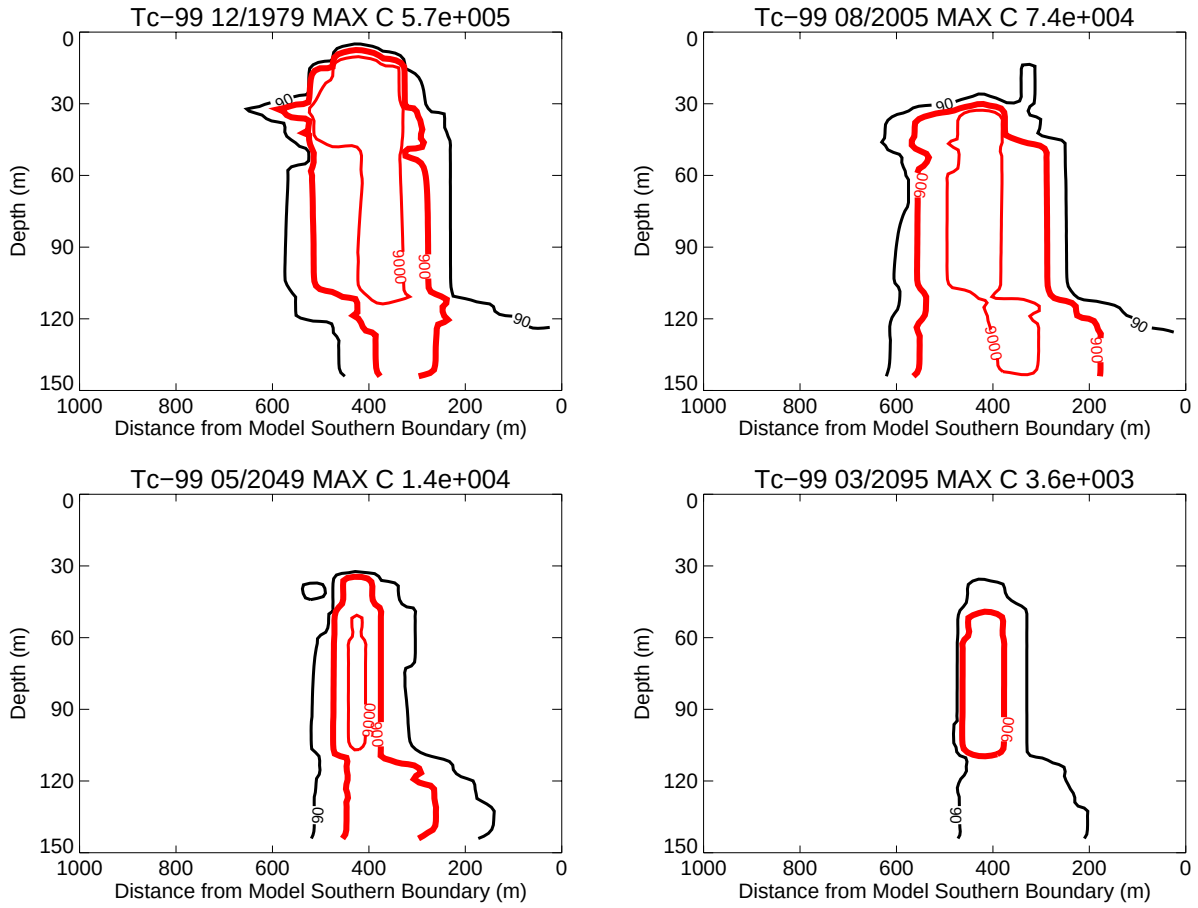

Figure A-10-49. Tc-99 vertical vadose zone concentrations (pCi/L) for the 50- x 50-m submodel case (MCL = thick red, MCL/10 = dotted, MCL*10 = thin red).

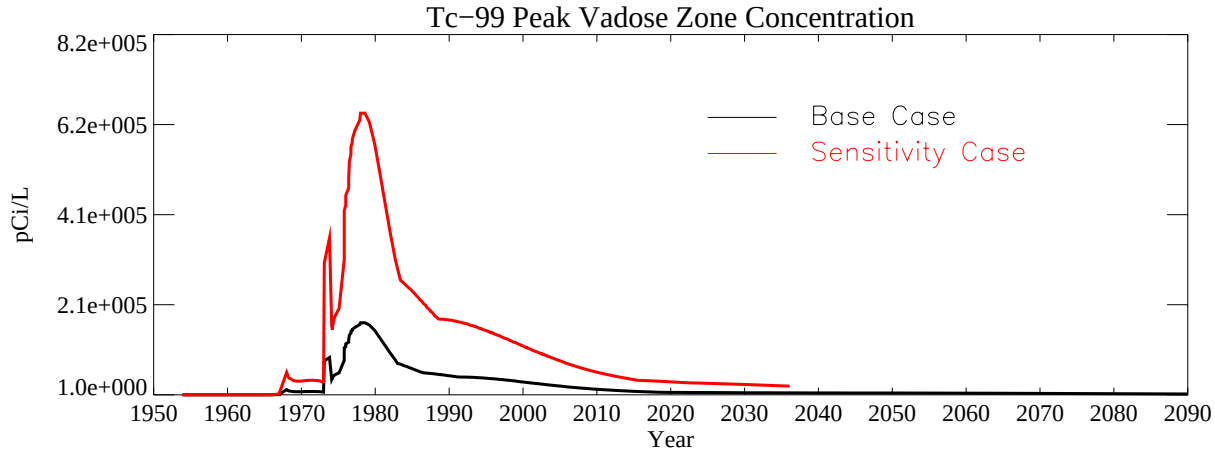

Figure A-10-50. Tc-99 peak vadose zone concentrations (excluding submodel area) (pCi/L) for the 50- x 50-m submodel case.

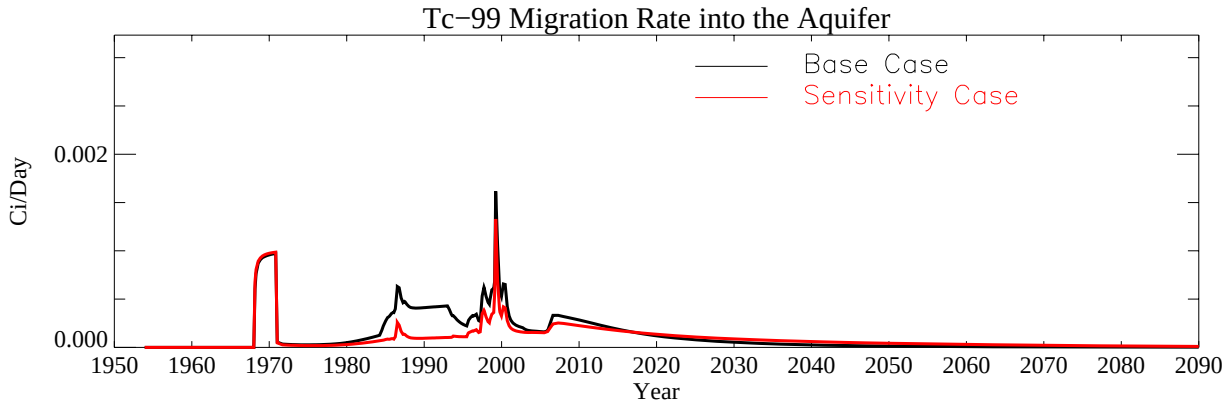

Figure A-10-51. Tc-99 flux into the aquifer (Ci/day) for the 50- x 50-m submodel case.

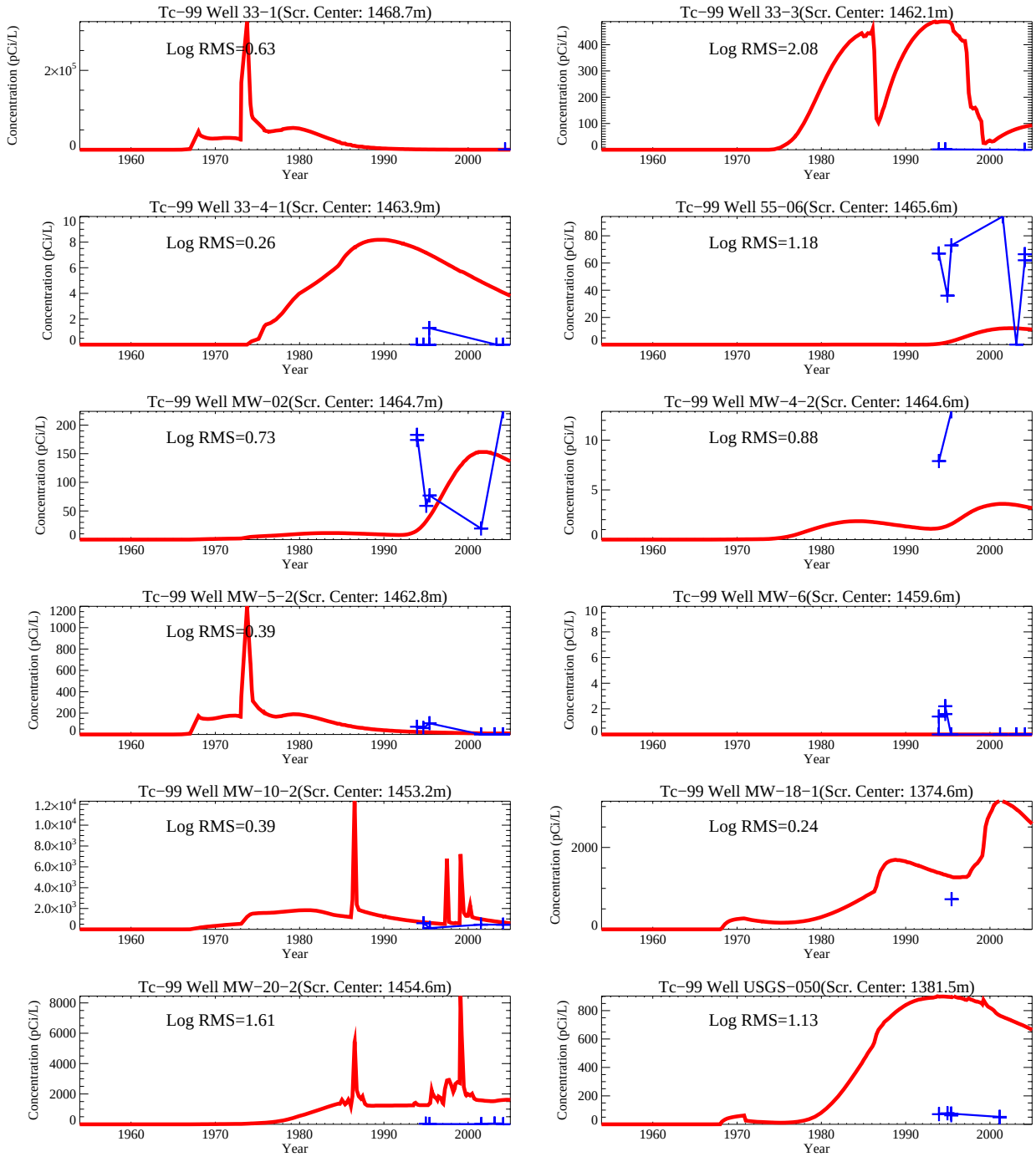

Figure A-10-52. Tc-99 concentration (pCi/L) in perched water wells for the 50- x 50-m submodel case (measured values = blue crosses, red = model at screen center).

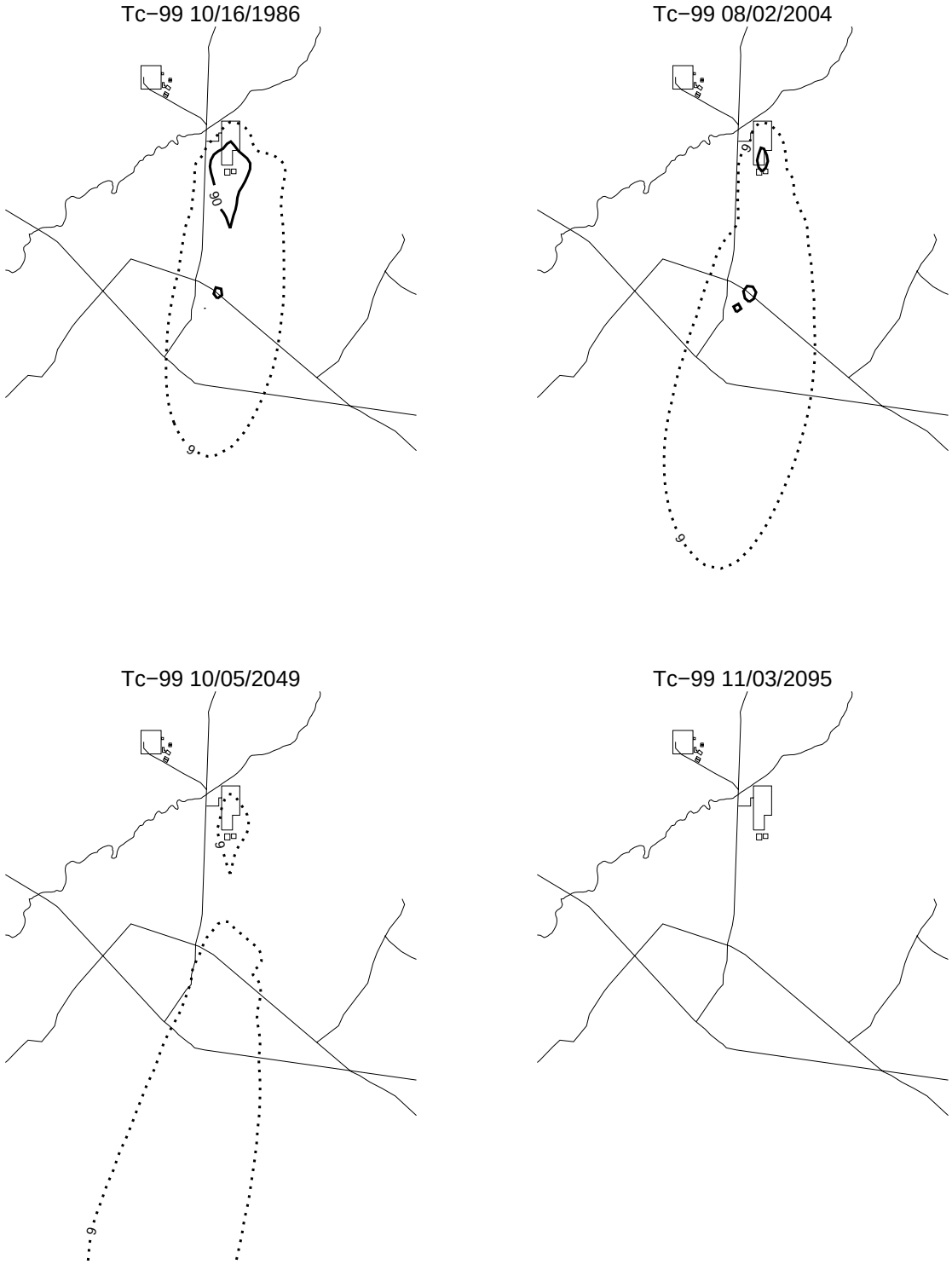

Figure A-10-53. Tc-99 aquifer concentrations (pCi/L) for the 50- x 50-m submodel case (MCL*10 = thin red, MCL = thick red, MCL/10 = thin black, MCL/100 = thin black dashed).

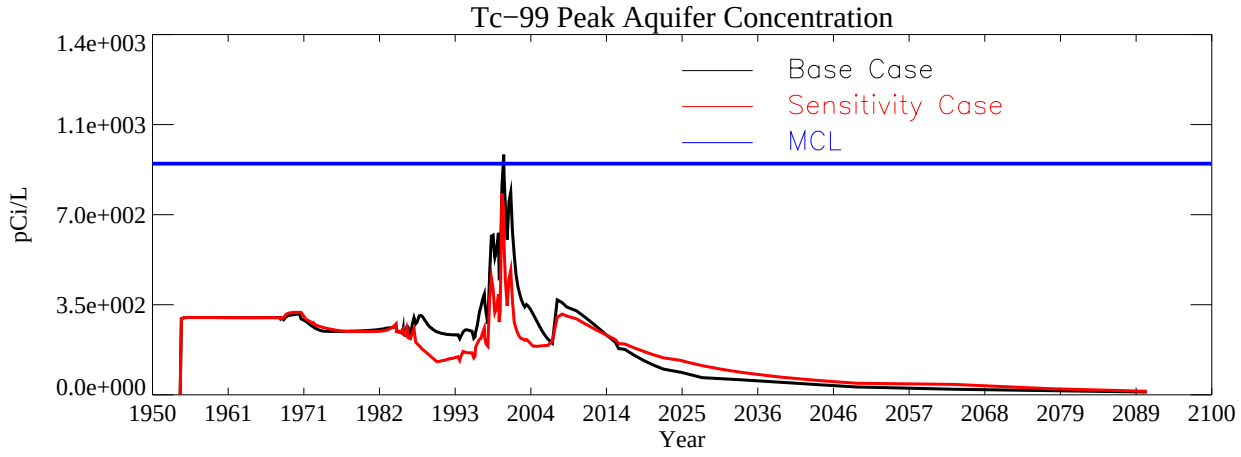

Figure A-10-54. Tc-99 peak aquifer concentration (pCi/L) for the 50- x 50-m submodel case.

A-10.1.6 Sensitivity Analysis Summary

Decreasing the tank farm recharge rate to 3 cm/year from 18 cm/year increases the travel time through the vadose zone and the peak Tc-99 concentrations by allowing a much longer and lower amplitude breakthrough to the aquifer. It also lessens the impact of the Big Lost River because less Tc-99 is deep in the vadose during the high flow years. Increasing the tank farm recharge to the maximum expected rate had a less dramatic effect than decreasing it to the minimum expected rate and did not significantly change the simulation results. This is because the recharge rate was only doubled, but the minimum expected rate decreased the recharge rate by a factor of six.

Tc-99 preferential flow path sensitivity simulations suggested a large fraction of the total tank farm Tc-99 must move from the 380-ft interbed directly to the aquifer near the ICPP-MON-A-230 well location to result in the high concentrations observed at this location. The peak Tc-99 concentrations in the 380-ft interbed were approximately 5,500 pCi/L in 1999 and a 10-gal/min flow rate from the 380-ft interbed resulted in a peak aquifer concentration of 3,842 pCi/L. The total amount of Tc-99 transferred from the 380-ft interbed at this flow rate was 2.87 Ci.

The highest and lowest interbed conductance simulations affected the influence of the Big Lost River and resulted in a lower amplitude and longer Tc-99 flux into the aquifer. The highest conductance interbed simulation reduced the horizontal spreading of the Big Lost River and allowed a smaller fraction of that flux to extend below the tank farm. The lowest conductance interbed simulation resulted in more horizontal spreading of the Big Lost River west of the tank farm but slightly less water reaching beneath the tank farm relative to the base case. However, agreement of the simulated and observed perched water concentrations was similar to the base case. The interbed conductance sensitivity simulations indicate that the model is more sensitive to interbed surface slope than permeability and thickness. Both the interbed conductance sensitivity realizations of the vadose zone lithology decreased the dip of the 140 ft interbed towards the tank farm and the resulting change in aquifer concentrations was similar.

Results of the horizontal discretization sensitivity simulations using smaller grid blocks resulted in higher concentrations, overprediction of concentrations in the nearest shallow perched water well (CPP-33-1), and underprediction of concentrations in the more distant wells (CPP-55-06 and MW-02). Matching the northern shallow perched water with the submodel would require a larger dispersivity value and the results would most likely be similar to the base case. This suggests the base case horizontal discretization was adequate to represent the vadose zone.

Table A-10-2 summarizes the sensitivity simulation results in the vadose zone and includes the peak concentration, time of peak, peak concentration in year 2005, and the peak concentration in the year 2095. Table A-10-3 presents the same information for the aquifer. Table A-10-4 presents the model calibration statistics for each sensitivity case and includes the average, minimum, maximum, and standard deviation of the log RMS for all vadose zone wells. The total number of simulated and observed pairs evaluated in calculating the calibration statistics is also included. This value is different for each sensitivity simulation because the log RMS was not calculated if simulated or observed values were zero. The statistics presented in Table A-10-4 allow evaluation of the agreement between the simulated and observed data. Sensitivity simulations that show a much worse agreement than the base case do not represent a true model sensitivity because the results are unrealistic.

Table A-10-2 Vadose zone model sensitivity analysis peak concentrations.

Section	Simulation	Year of Peak	Peak Concentration (pCi/L)	Peak Concentration in 2005 (pCi/L)	Peak Concentration in 2095 (pCi/L)
A-7.3.1	Tc-99 base case	1978	1.64e+5	1.91e+4	1.68e+3
A-10.1.2.1	Tc-99 high interbed conductance	1978	1.64e+5	2.61e+4	2.56e+3
A-10.1.2.2	Tc-99 low interbed conductance	1978	1.64e+5	2.71e+4	2.29e+3
A-10.1.3.1	Tc-99 3-cm/year tank farm recharge rate	1977	1.01e+6	5.47e+4	8.26e+3
A-10.1.3.3	Tc-99 39-cm/year tank farm recharge rate	1978	1.49e+5	7.60e+3	1.69e+3
A-10.1.3.4	Tc-99 maximum anthropogenic water recharge rate	1978	3.34e+4	7.60e+3	1.69e+3
A-10.1.4.1	Tc-99 10-gal/min preferential flow path from 380-ft Interbed[a]	1978	1.64e+5	1.91e+4	1.68e+3
A-10.1.5.2	Tc-99 estimate from 25.1 Tc-99/ I-129 ratio	1978	1.64e+5	1.91e+4	1.68e+3
A-10.1.6.1	Tc-99 50- x 50-m horizontal grid	1978	6.41e+5	7.40e+4	3.64e+3

a. Identical to base case.

Table A-10-3 Aquifer model sensitivity analysis peak concentrations.

Section	Simulation	Year of Peak	Peak Concentration (pCi/L)	Peak Concentration in 2005 (pCi/L)	Peak Concentration in 2095 (pCi/L)
A-8.3.2	Tc-99 base case	1999	935	234	11
A-10.1.2.1	Tc-99 high interbed conductance	1999	568	203	43
A-10.1.2.2	Tc-99 low interbed conductance	1999	628	169	45

Section	Simulation	Year of Peak	Peak Concentration (pCi/L)	Peak Concentration in 2005 (pCi/L)	Peak Concentration in 2095 (pCi/L)
A-10.1.3.1	Tc-99 3-cm/year tank farm recharge rate	1999	327	125	40
A-10.1.3.3	Tc-99 39-cm/year tank farm recharge rate	1999	970	220	10
A-10.1.3.4	Tc-99 maximum anthropogenic water recharge rate	1986	799	139	22
A-10.1.4.1	Tc-99 10 gal/min preferential flow path from 380-ft interbed	1986	3,842	307	9
A-10.1.5.2	Tc-99 estimate from 25.1 Tc-99/ I-129 ratio	1999	935	236	15
A-10.1.6.1	Tc-99 50- x 50-m horizontal grid	1999	783	192	14

Table A-10-4 Vadose zone model sensitivity analysis calibration statistics.

Section	Simulation	Average Log RMS Error	Minimum Log RMS Error	Maximum Log RMS Error	Standard Deviation Log RMS Error	Number of Pairs Evaluated
A-7.3.1	Tc-99 base case	1.14	0.193	2.81	0.603	54
A-10.1.2.1	Tc-99 high interbed conductance	0.984	0.0141	2.89	0.722	56
A-10.1.2.2	Tc-99 low interbed conductance	0.972	0.154	2.84	0.648	56
A-10.1.3.1	Tc-99 3-cm/year tank farm recharge rate	1.09	0.359	2.96	0.638	56
A-10.1.3.3	Tc-99 39-cm/year tank farm recharge rate	1.02	0.057	2.54	0.613	56
A-10.1.3.4	Tc-99 maximum anthropogenic water recharge rate	0.933	0.0304	2.91	0.634	56
A-10.1.4.1	Tc-99 10-gal/min preferential flow path from 380-ft interbed[a]	1.14	0.193	2.81	0.603	54
A-10.1.5.2	Tc-99 estimate from 25.1 Tc-99/ I-129 ratio	1.17	0.193	2.81	0.594	54
A-10.1.6.1	Tc-99 50- x 50-m horizontal grid	0.639	0.241	2.08	0.681	46

a. Identical to base case.

A-10.2 Model Uncertainty Analysis

Prediction uncertainty is comprised of (1) uncertainty in the conceptual model (i.e., a complex process oversimplified or not well understood) and (2) a lack of knowledge about the model parameter values. The conceptual model uncertainty can be qualitatively assessed by comparing simulation results to observations and assessing whether sufficient complexity exists to capture the observed behavior. Parametric uncertainty can be quantitatively assessed by using Monte Carlo simulation if sufficient data exist to define probability distributions for all parameters. This was not done here because (1) there are insufficient data to create probability distributions of the model parameters and (2) the most sensitive model parameters were adjusted to minimize the mismatch between prediction and observations during the model calibration process. The model's parametric uncertainty is qualitatively presented in the context of the sensitivity analysis results.

The primary purpose of the OU 3-14 model is to predict future Snake River Plain groundwater concentrations from the tank farm soil sites and to evaluate proposed remedial actions. Numerical simulation of aquifer and vadose zone transport is inherently uncertain because observations of subsurface conditions are very sparse as are the data gathered to parameterize the model. This section is included to discuss these uncertainties in context of the primary purpose. Conceptual model uncertainty is assessed in Section A-10.2.1, Section A-10.2.2 presents the parametric uncertainty, and Section A-10.2.3 summarizes the model uncertainty for each contaminant of concern simulated as being low, moderate, or high.

A-10.2.1 Conceptual Model Uncertainty

The uncertainty due to model conceptualization is assessed in terms of how successful the calibration was in matching the observed data. A good agreement between model and observations indicates the conceptual model included sufficient complexity to match the actual behavior and the modeled system was well understood. A summary of the model calibration is provided in this section to provide a basis for assessing the conceptual model uncertainty.

The conceptual model adopted for the INTEC vadose zone attributes surface recharge to the transient Big Lost River, uniformly distributed steady-state precipitation, and time-varying anthropogenic water sources. The magnitude of these recharge sources are larger than exist across the INL Site as a whole. Increased recharge in the INTEC area infiltrates downward through a heterogeneous vadose zone comprised of the alluvium; fractured basalt; and 110-ft, 140-ft, below middle massive basalt (BM), and 380-ft interbeds. There are additional discontinuous sediment units interspersed between these primary lithologic units. Near land surface, liquid spills have occurred, releasing contaminants into the environment. We have assumed that these spills occurred uniformly in time over the estimated release period. Contaminants are then allowed to partition onto the soil, and this partitioning is described using a linear sorption isotherm. Subsequent transport occurs under spatially and temporally varying conditions as the contaminants migrate downward to the aquifer. The ability of the OU 3-14 conceptual model to represent these subsurface conditions is illustrated in the vadose zone and aquifer model calibration sections (Sections A-7 and A-8, respectively).

The simulated recharge originating in the former percolation ponds and the Big Lost River resulted in the formation of extensive perched water bodies beneath these location. The simulated perched water occurs within and above the major interbeds and is consistent with observed perched water near the Big Lost River and below the former percolation ponds. The areal extent of the perched water below the percolation ponds is consistent with the observed extent and did not reach much beyond the MW-7 well. This extent is consistent with the geochemical analysis presented in the MWTS report (DOE-ID 2003a). The recharge from precipitation and facility-related discharges resulted in very high saturation (0.99) in the low-permeability interbeds beneath INTEC, but the water phase pressure is slightly negative. This is consistent with the ephemeral perched water behavior observed in many of the wells beneath the INTEC, but not all locations. A very high interbed saturation would result in the perched water screens behaving as a seepage face and resulting in only small amounts of water being able to be withdrawn without the well temporarily drying out. The locations of the simulated high saturation areas agree with the observed perched water locations. However,

some observed perched water locations beneath the northern INTEC and away from the Big Lost River contain substantial perched water depth and even have rapid lateral flow.

The simulated recharge from the Big Lost River and former percolation ponds resulted in perched water and positive water phase pressure in these locations. The observed perched water drained out after the percolation ponds were relocated in 2002, and this behavior is generally captured by the model. The agreement between simulated and observed perched water suggests that the OU 3-14 vadose zone conceptual model is sufficient and the uncertainty is acceptable, but it is not low because the model did not create positive water at the perched water locations near the tank farm.

The highest observed contaminant concentrations in the northern shallow perched water are located south, east, and southeast of the tank farm in wells CPP-33-1, MW-2, MW-10-2, MW-20-2, MW-5, and CPP-55-06. This was presented for both predicted and observed data in Section A-7.3. The model is consistent with this observed trend.

The simulated transport of Tc-99 from the tank farm release sites resulted in peak aquifer concentrations occurring in the year 1999. The highest measured aquifer concentrations were found in the first sampling of the ICPP-MON-A-230 in 2003. The observed aquifer concentrations in other aquifer wells near the tank farm suggest that Tc-99 concentrations in the aquifer have been either changing slowly or steady since the mid 1990s. However, there are insufficient data for conclusive model calibration to deep vadose zone or aquifer peak concentrations. Conclusive model calibration requires knowledge of the source and concentration history in observation wells. Most often, the perched water wells were monitored after the majority of Tc-99 passed the monitoring locations or the sampling period was too short to discern where on the concentration history the data lie.

Steady-state underflow is assumed to move beneath the INTEC through the fast-moving aquifer and recharge and contaminants from the vadose zone water are diluted and dispersed as they slowly percolate downward. The model includes the INTEC production and injection wells as sinks and sources at the well screen depths. The aquifer thickness was estimated based on deep well temperature profiles and is spatially varying. The aquifer model included the following three lithological layers: (1) H basalt from the water table to the HI interbed with permeability estimated from aquifer well test data, (2) HI interbed with permeability estimated from laboratory testing of core, and (3) I basalt with permeability estimated based on fitting the tritium, I-129, and Sr-90 data.

The simulated large-scale aquifer gradient near the INTEC is mostly due south. This matches the large-scale regional gradient predicted in the summer 2004 water level measurements. The aquifer model had good agreement with observed contaminant arrival in downgradient wells for contaminants discharged into the CPP-3 injection well. There are sufficient time histories for contaminants to discern the rising limb, peak concentration, and falling limb of the tritium and Sr-90 concentrations in the observed concentration histories. The agreement with the simulated and observed large-scale gradient and contaminant history data (specifically tritium) indicate that the OU 3-14 aquifer model has sufficient complexity to match the observed water behavior and the uncertainty is acceptable. The relatively poor match with Sr-90 concentrations in the aquifer suggest spatially varying sorption chemistry is occurring within the aquifer and the model does not contain this complexity/understanding. For this reason, the conceptual model uncertainty within the aquifer is only acceptable.

A-10.2.2 Parametric Uncertainty

The model parametric uncertainty analysis quantifies the model output uncertainty to the model's input parameters. The results of the sensitivity analysis forms most of the basis for the parametric uncertainty discussion presented in this section. The OU 3-14 source term was not included in the sensitivity analysis, but the OU 3-14 source term is an important model parameter and the uncertainty is discussed in this section. Contaminant transport scales linearly with an increase or decrease in source magnitude, and a linear increase or

decrease in the OU 3-14 source terms would result in a corresponding linear increase in the predicted groundwater concentrations.

In general, the most sensitive parameters suggest highest uncertainty. However, this is qualified here: If the sensitivity analysis was high for a specific parameter and that specific parameterization resulted in a greatly increased mismatch between observed and predicted data, the uncertainty is less than suggested by the sensitivity analysis. The parameters contributing most to uncertainty are (1) the source terms, (2) model transport parameters, (3) model hydraulic parameters, (4) infiltration rate, and (5) subsurface structure. Each of these are discussed in the next sections.

A-10.2.2.1 Contaminant Source Terms

The source terms used in the groundwater risk assessment included (1) the tank farm leaks and spills that created the OU 3-14 contaminated sites, (2) the service waste disposed of into the former CPP-3 injection well and percolation ponds, and (3) OU 3-13 soil sites. The uncertainty of each source is presented below. The service waste (except Tc-99) and the OU 3-13 soil sites source terms were taken from the OU 3-13 RI/FS (DOE-ID 1997), and much of the uncertainty discussion was taken from the OU 3-13 RI/FS.

A-10.2.2.1.1 OU 3-14 Sources

The source term uncertainty for most of the smaller tank farm sites is of no consequence because the activity released was insignificant compared to the few large releases. In the tank farm, there was one major release (CPP-31); three much lower and roughly equal releases (CPP-79 [deep]; CPP-27/31; and CPP-28); and several other minor releases that had a total activity several orders of magnitude lower than the four largest releases. Releases incorporated in the model included both measured and estimated waste volumes and waste compositions. The measured values are expected to be more accurate than the estimated values.

There are two main areas of uncertainty in the waste source terms: first is the volume of waste released; second is the activity per unit volume of waste released. The uncertainty in the specific activity varies among the radionuclides. In general, the activity of the fission products (Cs-137, Sr-90, Tc-99, etc.) can be accurately (within 5%) estimated or measured. Tritium and I-129 can be accurately measured or estimated in some wastes. However, due to their volatility, those radionuclides sometimes separate from the bulk of the fission products. When this occurs, the estimates become less accurate. The activity of the activation products (including the transuranic components) can be accurately measured, but estimates of the activation products are less accurate than those of the fission products due to difference in fuel design, reactor operation, etc., that affect the activity of activation products. The estimates of the activation products may be accurate within a factor of two.

In addition to the radionuclide activities, the waste compositions include nitrate concentrations. The nitrate concentrations for the major releases are either measured or estimated based upon waste generation and treatment flowsheets. Most of the nitrate estimates are likely accurate to within 20%. The nitrate concentrations are inherently more accurate than many of the radionuclide activities because of process and physical limits (solubility) on the nitrate concentration.

The uncertainty of each major release site is presented in the following:

- **CPP-31** – This is the source of the bulk of activity released at the tank farm. The uncertainties in its source term are larger than many of the other source terms. The CPP-31 source term (total activity) is an order of magnitude higher than even the second largest tank farm release source term. The volume of waste released was estimated to be 18,600 gal. This value is good to plus/minus 4,000 gal (about 20%). The radionuclide activity included measured values from waste sample analyses (variability of 10% or less) for Cs-137, Sr-90, H-3, U, Pu, and nitrate.

  Tc-99 was not measured but is expected to be accurately estimated based upon fission yield. The waste

had been concentrated in the process equipment waste evaporator, which depleted the H-3 and I-129 from the fission yield values. Therefore, the estimated I-129 activity was reduced by the same factor as the measured H-3 activity. This is probably accurate to within a factor of two for I-129. Other transuranic components (Np-237, Am-241, etc.) are likely within a factor of two, based on the ORIGEN2-based estimates documented in Appendix E.

- **CPP-27/33** – This leak consisted of Waste Calcining Facility scrub solution. In this case, neither the volume nor composition was measured at the time of the release. However, most of the contaminated soil was removed and the activity of Cs-137 in the contaminated soil was measured/estimated. A reasonable Waste Calcining Facility scrub solution activity was assumed (based on historical sample data), and the total Cs-137 activity released was divided by the Waste Calcining Facility scrub solution Cs-137 specific activity to get the volume of scrub solution released. In this case, the waste activity and waste volume do not have separate uncertainties. An error in one tends to be cancelled by a compensating error in the other. For example, if the assumed specific activity is too low, then the calculated waste volume is too high by a compensating percentage (and visa versa). Therefore, although errors are likely in both the activity and waste volume estimates, they are not necessarily additive. In this case, the greatest uncertainty lies with the estimate of the total Cs-137 activity in the soil that was removed. However, the model does not account for soil removal.

  The Cs-137 activity was estimated based upon average radiation readings taken from five (accessible) sides of the waste boxes as the soil was removed from the site in 1974. Basing the Cs-137 on such readings is likely accurate to within a factor of two. All other radionuclides were calculated based upon Cs-137; therefore, most fission products will be accurate to a factor of two. Due to their volatility, the H-3 and I-129 estimates may be less accurate than other fission products. The activation products are also likely good to a factor of two because they were a long-term average of fairly well-defined waste (first-cycle Al raffinate).

  The nitrate estimate for this release is not as good as other releases because the release consisted of two parts: (1) a high-activity stream for which the nitrate estimate is very good and (2) a low-activity (decon solution) stream for which the nitrate concentration estimate is good, but the volume is unknown. The second waste stream does not affect the radionuclide activity. In this case, the nitrate is likely good to only a factor of two as well.

- **CPP-28** – This leak consisted of first-cycle coprocessing raffinate. Such waste was well defined. The specific activity of the waste was based upon contemporary analyses of coprocessing wastes that included Cs-137, Sr-90, H-3, U, Pu, and Np-237. Tc-99 and I-129 were not included in the analyses but can be accurately estimated based upon fission yield. The specific activity estimate of these radionuclides is good. The activation products transuranics were estimated based upon the Cs-137 activity. The volume of waste released was estimated based upon the volume of contaminated soil, activity of the soil, and the specific activity of the waste. As with CPP-27/33, errors in the estimated volume released are somewhat compensated by the errors in the source term specific activity. If the estimated specific activity is too high, the estimated volume will be too low. So the errors in activity and volume are not additive. The major source of error is in the total activity originally in the contaminated soil. The total error (combined volume and specific activity) is accurate to about 50% for the fission products and a factor of two for the activation products.

- **CPP-79 (deep)** – This release is the least well defined of the four major tank farm releases and thus has the most uncertainty. The activity released was based upon blends of predominantly stainless-steel, first-cycle raffinate, with smaller amounts of Al, Zr, and other wastes. The fission product estimates are likely very accurate relative to each other (within 5%). Due to the blending of wastes, the activation product activity could vary significantly. However, all activity depends upon the estimate of the Cs-137 activity. The waste that leaked was assumed to have been first-cycle raffinate. In fact, a significant

portion of the waste was not first-cycle raffinate. Such waste would have a significantly lower Cs-137 activity. The estimated leak volume was based upon steam dilution estimates of waste transfers. Steam jet dilution is variable and those estimates could be off by a factor of two.

Although the total activity estimate for CPP-79 (deep) is potentially more variable than other releases, the assumption and estimates were on the conservative (high-activity) side. The ORIGEN simulations generated two potential waste source terms, based upon different blends of waste. Both estimates have similar fission product activity, but the transuranic content varies by about a factor of two (some slightly more, some slightly less). The stream with the highest Pu-239 activity was used, and the entire release was assumed to be first-cycle raffinate. This assumption is not correct because a portion of the waste released was not first-cycle raffinate but included some relativity process equipment waste solution and perhaps other relativity solution. Therefore, although the specific activity is variable, the fission product activity could be no more than 25% higher, but it could be considerably less (up to a factor of two). Likewise, the transuranic activity is likely no more than a factor of two higher than the estimate, but could be up to a factor of four less.

A-10.2.2.1.2 Service Waste

The injection well provided a direct source of contamination to the aquifer. However, during the injection well failure, a large fraction of the service waste stream entered the vadose zone. During this period, the depth of the discharge to the vadose zone is uncertain. The vadose zone disposal of the service waste could result in a delayed arrival to the aquifer and allow the contaminants to arrive in the aquifer after the well was repaired and receiving service waste again. This could result in a short period of higher concentrations due to superposition of the delayed and current disposal. The vadose zone and aquifer models should capture the behavior because, during the estimated well failure period, the injection well disposal was placed into the vadose zone model.

The discharges of H-3 and Sr-90 to the service waste stream were monitored regularly and the uncertainty in these two contaminant source terms should be small. The discharge of I-129 was also monitored but less frequently than H-3 and Sr-90. The source term for the other COPCs was estimated from less data and the uncertainty is higher. The H-3 and Sr-90 were regularly monitored in the downgradient wells and provide a check of the uncertainty in these two source terms. The aquifer model had good agreement with the observed H-3 and Sr-90 and verifies the uncertainty is not significant for these two COPCs.

The Tc-99 concentrations were never monitored in the INTEC service waste. The service waste source term was estimated from 2001 Tc-99-to-I-129 concentration ratios in the aquifer near the CFA and the I-129 source term (see Section A-9.2.3). The sensitivity of the model to an increased Tc-99 service waste was evaluated by using the maximum Tc-99-to-I-129 ratio to estimate the source term and can be used to assess effect of the Tc-99 service waste uncertainty. The uncertainty of the injection well Tc-99 source term will result in higher or lower concentrations far south of INTEC at the current time and should not significantly change predicted concentrations near INTEC now or into the future. The uncertainty of the other COPCs is recognized but cannot be quantified.

The arrival of each OU 3-14 tank farm COPC to the aquifer should occur long after the injection well component of that COPC has moved south of INTEC. This should not allow superposition of each COPC when evaluating whether the COPC is above the MCL, but superposition of different COPCs can occur for a risk calculation. Most of the Sr-90 currently in the aquifer beneath INTEC is the result of the CPP-3 injection well operation and will contribute to a higher cumulative risk as unretarded tank farm COPCs arrive in the aquifer. Thus, the injection well source term uncertainty would only contribute to total risk calculations from the tank farm sources and should not contribute to an MCL evaluation for each COPC, because the CPP-3 injection well source will have moved south of INTEC before the tank farm sources reach the aquifer.

As with the CPP-3 injection well, the former percolation pond sources were estimated from discharge records reported for the percolation ponds. The discharge records were not regularly reported over the years,

and an average daily discharge was used for the percolation ponds source terms. The uncertainty of the percolation pond source terms is recognized but cannot be quantified.

A-10.2.2.1.3 OU 3-13 Soil Sources

The OU 3-13 soil sources were estimated from the volume and contaminated soil concentration. These sources were implemented in the model on March 29, 1990, and represent radioactivity remaining in the soil at this time. The contaminated soil volume was assumed to be represented by a cube spanning the horizontal extent of measured contaminant and extending from land surface to the top of basalt. The soil concentration applied to this soil volume was typically the highest measured value. Using the spanning volume and maximum concentrations means that both the soil volume and concentration were conservatively estimated and that the total radioactivity assumed to be at each site is most likely much less. The uncertainty in the soil sources will result in overestimating the contribution to groundwater risk from these locations.

A-10.2.2.2 Transport Parameters

Simulating contaminant transport through porous media requires parameterizing the solute chemical interaction with the soil/rock matrix (sorption) and dispersion in the modeled system. The model's sensitivity to sorption and dispersivity were investigated simulating Sr-90 and is presented in Appendix J.

A-10.2.2.3 Hydraulic Parameters

Numerous cores of INTEC sediment have been taken, and laboratory analysis of the cores has been performed to estimate hydraulic conductivity, porosity, and soil moisture characteristics. However, hydrologic parameters tend to be scale-dependent. Cores represent nearly point-scale data, and the model represents a field scale. The model can be parameterized with the measured hydraulic properties, but disparity between measured and simulated scales requires adjustment of parameters to match observed conditions. The model was calibrated to perched water elevation, perched water temporal trends, and contaminant concentrations in the perched water and aquifer. The calibration process should reduce the model's uncertainty due to hydraulic parameters to a small amount.

A-10.2.2.4 Infiltration Rate

The model's infiltration rate was spatially varying and was estimated from known anthropogenic sources (i.e., lawn irrigation, steam vents, and line leaks) and from the natural water sources (i.e., Big Lost River and precipitation). There is a large amount of uncertainty in the amount and locations of the anthropogenic water sources and the recharge from precipitation because of the following reasons: (1) approximately 10-11% of the produced water is unaccounted for, (2) the accuracy of the flow meters on the production wells is unknown, and (3) very limited soil moisture data were used to estimate infiltration due to precipitation. The model's sensitivity to infiltration was investigated for a long-lived mobile contaminant (Tc-99) and for a short-lived relatively immobile contaminant (Sr-90, see Appendix J) for a high and low tank farm infiltration rate, and, for a worst case, anthropogenic infiltration rate.

The model's Tc-99 sensitivity to different infiltration rates was not great because a large fraction of the Tc-99 inventory was directly injected to the aquifer in the CPP-3 disposal well. This is probably a real source of uncertainty in the model predictions because the agreement between the simulated and observed perched water was comparable and either simulation could equally represent Tc-99 contaminant transport. The peak Tc-99 arrival in the northern shallow perched water was not observed in the field data and the higher and lower infiltration rates were in the tail of the observed data. Peak aquifer concentrations were within a factor of two to three of the base case and the uncertainty is acceptable.

The Sr-90 uncertainty due to infiltration rates is substantially greater because changes in vadose zone water velocity are multiplied by the retardation factor, and the average Sr-90 travel time through the vadose zone is several half-lives (see Appendix J).

A-10.2.2.5 Subsurface Structure

The INTEC subsurface is a highly complex layering of basalt flows and sedimentary interbeds, and an infinite number of possible structures could be inferred from the well log data. The sensitivity analysis used the most conducive for transport and least conducive for transport generated using stochastic simulation to evaluate model sensitivity to subsurface structure. The two structures were run with Sr-90 and Tc-99.

As with the infiltration rate sensitivity, the Tc-99 sensitivity to different subsurface structures was not great because a large fraction of the Tc-99 inventory was directly injected into the aquifer at the CPP-3 disposal well. This is probably a real source of uncertainty in the model predictions because the agreement between the simulated and observed perched water was comparable and either simulation could equally represent Tc-99 contaminant transport. Peak aquifer concentrations in the year 2095 were higher than the base case, but still an order of magnitude below the MCL.

A-10.2.3 Model Uncertainty Summary

The possible impact of the uncertainty is summarized for each COPC simulated in the groundwater risk pathway (except Sr-90, which may be found in Appendix J) as follows:

- **H-3** – The majority of the H-3 released to the INTEC subsurface originated from the CPP-3 injection well. The injection well contributed 20,100 Ci and the OU 3-14 tank farm sources contributed only 10 Ci out of a total 21,500 Ci released to the subsurface. Uncertainty due to vadose zone model parameters, vadose zone model structure, net infiltration rate, and tank farm source terms is insignificant. The aquifer model was calibrated to tritium concentrations in monitoring wells, and tritium discharges to the service waste water were monitored regularly. The tritium concentrations in downgradient wells were also regularly monitored. The overall uncertainty in the tritium aquifer concentrations predictions is low.

- **I-129** – The majority of the I-129 released to the INTEC subsurface also originated from the CPP-3 injection well. The injection well contributed 0.86 Ci and the OU 3-14 tank farm sources contributed only 0.001 Ci out of a total 0.98 Ci released to the subsurface. Uncertainty due to vadose zone model parameters, vadose zone model structure, net infiltration rate, and tank farm source terms is insignificant. The aquifer model was not calibrated to aquifer I-129 concentrations but was compared to observed concentrations. The simulated and observed concentrations were similar. I-129 discharges into the service waste stream and aquifer concentrations were monitored less frequently than tritium. The overall uncertainty in the I-129 predictions of groundwater concentration is low for sources originating from the injection well and the tank farm.

- **Np-237** – The majority of the Np-237 released to the INTEC subsurface also originated from the CPP-3 injection well. The CPP-3 injection well contributed 1.07 Ci and the OU 3-14 tank farm sources contributed only 0.03 Ci out of a total 1.2 Ci released to the subsurface. Uncertainty due to vadose zone model parameters, vadose zone model structure, net infiltration rate, and tank farm source terms is small. Np-237 discharges to the service were monitored infrequently and were estimated using process knowledge. The overall uncertainty in groundwater concentration prediction from Np-237 is moderate.

- **Pu-239** – The majority of the Pu-239 released into the INTEC subsurface originated from the OU 3-14 tank farm sources and the OU 3-13 soil contamination sites. The OU 3-14 sources contributed 6.9 Ci and the OU 3-13 soil contamination sites contributed 1.1 Ci out of 8.0 Ci released to the subsurface. The CPP-31 was the largest contributor to the Pu-239 inventory, which was estimated to be accurate within 30% (20% in liquid volume and 10% in activity concentration). Pu-239 is highly retarded in the subsurface and the travel time was estimated to be 90,000 years. The source uncertainty for Pu-239 is low, but the very long vadose zone travel time increases the predictive uncertainty and the overall uncertainty in groundwater concentration prediction is high. The uncertainty of exceeding the MCL is

low because the maximum predicted concentration is several orders of magnitude below the MCL.

- **Pu-240** – The majority of the Pu-240 released into the INTEC subsurface originated from the OU 3-14 tank farm sources and the OU 3-13 soil contamination sites. The OU 3-14 sources contributed 1.07 Ci and the OU 3-13 soil contamination sites contributed 0.12 Ci out of 1.2 Ci released to the subsurface. The Pu-240 source term uncertainty and vadose zone transport uncertainty are the same as that for Pu-239. The uncertainty for the Pu-240 prediction is high. The uncertainty of exceeding the MCL is low because the maximum predicted concentration is several orders of magnitude below the MCL.

- **Tc-99** – The majority of the Tc-99 released into the INTEC subsurface originated from the CPP-3 injection well, but the OU 3-14 tank farm source also contributed a significant fraction. The CPP-3 injection well contributed 11.9 Ci and the OU 3-14 tank farm source contributed 3.56 Ci out of 16.7 Ci released to the subsurface. The majority of the tank farm source is from the CPP-31 site and the source was estimated to be accurate within 30%. However, the CPP-3 injection well source was estimated from aquifer concentration ratios of I-129 to Tc-99 and the I-129 source. The calibration of the vadose zone model to the observed Tc-99 concentrations in the northern shallow perched water wells is uncertain because the data began after peak concentrations of Tc-99 had passed through. The aquifer model also underpredicts the concentrations at the ICPP-MON-A-230 well. For these reasons, the uncertainty of the Tc-99 prediction is high.

- **U-234** – The OU 3-14 tank farm sources, OU 3-13 soil contamination sources, and the CPP-3 injection well all contributed similar amounts to the total U-234 released to the subsurface. The OU 3-14 tank farm sources contributed 0.095 Ci, the OU 3-13 soil contamination sources contributed 0.140 Ci, and the injection well contributed 0.135 Ci out of 0.391 Ci released to the subsurface. The majority of the tank farm source is from the CPP-31 site and the source was estimated to be accurate within 30%. The OU 3-13 soil site sources were estimated to be grossly conservative. The injection well U-234 was estimated from very limited data. U-234 is retarded in the subsurface, but the half-life is 244,000 years and radioactive decay en route to the aquifer is negligible. Thus, uncertainty in the radioactive decay attenuation en route to the aquifer is negligible. However, the source term is believed to be overpredicted because of the grossly high OU 3-13 estimates and an overestimated OU 3-14 source term. The overall uncertainty of the U-234 groundwater concentration prediction is moderate because of the uncertainty in the injection well source term and conservative OU 3-13 and OU 3-14 source terms. The uncertainty of exceeding the MCL is low because the maximum predicted concentration is several orders of magnitude below the MCL.

- **Mercury** – The majority of the mercury released into the subsurface originated from the OU 3-13 soil sources and CPP-3 injection well. The OU 3-13 soil sources contributed 585 kg and the injection well contributed 400 kg. The OU 3-14 tank farm sources only contributed 72 kg. The injection well source term was estimated and the OU 3-13 soil site source term was grossly overestimated and was equal to that used for the OU 3-13 RI/BRA. As a result, the overall uncertainty of the mercury groundwater concentration prediction is high. The uncertainty of exceeding the MCL is low because the maximum predicted concentration after 2095 is an order of magnitude below the MCL and the OU 3-13 sources were grossly overestimated.

- **Nitrate** – The majority of the nitrate released into the INTEC subsurface originated from the CPP-3 injection well and the former percolation ponds. The injection well contributed 2,830,000 kg; the former percolation ponds contributed 1,310,000 kg; and the OU 3-14 tank farm sources only contributed 21,200 kg out of a total 4,160,000 kg released into the subsurface. Uncertainty due to vadose zone model parameters, vadose zone model structure, net infiltration rate, and tank farm source terms is insignificant. The aquifer model was not calibrated to aquifer nitrate concentrations but was compared to observed

concentrations. The simulated and observed concentrations were similar. The overall uncertainty in the nitrate prediction of groundwater concentration is low.

A-11 REFERENCES

Ackerman, D. J., 1991, "Transmissivity of the Snake River Plain Aquifer at the Idaho National Engineering Laboratory Idaho," U.S. Geological Survey-Water Resources Investigations Report 91-4058.

Anderson, S. R. and B. D. Lewis, 1989, "Stratigraphy of the Unsaturated Zone at the Radioactive Waste Management Complex, Idaho National Engineering Laboratory, Idaho," U.S. Geological Survey Water-Resources Investigations Report 89-4065, IDO-22080.

Anderson, S. R., 1991, "Stratigraphy of the Unsaturated Zone and Uppermost Part of the Snake River Plain Aquifer at the Idaho Chemical Processing Plant and Test Reactors Area, Idaho National Engineering Laboratory, Idaho," U. S. Geological Survey Water-Resources Investigations Report 91-4010.

Bear, J., 1972, *Dynamics of Fluids in Porous Media*, New York: American Elsevier Publishing.

Bennett, C. M., 1990, "Streamflow Losses and Ground-Water Level Changes Along the Big Lost River at the Idaho National Engineering Laboratory, Idaho," DOE/ID-22091, U.S. Geological Survey Water-Resources Investigations Report 90-4067.

Brooks, R. H. and A. T. Corey, 1966, "Properties of Porous Media Affecting Fluid Flow," *J. Irrig. Drain. Div*., Am Soc. Civil Eng., Vol. 92 (IR2), pp. 61-88.

Buckham, J. A., to C. W. Bills, Atomic Energy Commission, October 12, 1970, "Liner Construction Materials CPP No. 3 Injection Well," Buc-312-70.

Cahn, L. S., and S. L. Ansley, 2004, *Analysis of Perched Water Data from ICDF Monitoring Wells*, INEEL/EXT-03-00250, Rev. 0, Idaho National Engineering and Environmental Laboratory, Idaho Completion Project, September 2004.

DOE-ID, 1994, *Track 2 Sites: Guidance for Assessing Low Probability Hazard Sites at the INEL*, DOE/ID-10389, Rev. 6, U.S. Department of Energy Idaho Operations Office, January 1994.

DOE-ID, 1997, *Comprehensive RI/FS for the Idaho Chemical Processing Plant* OU *3-13 at the INEEL, Part A, RI/BRA Report (FINAL),* U.S. Department of Energy Idaho Operations Office, DOE/ID-10534, November 1997.

DOE-ID, 1999, *Final Record of Decision Idaho Nuclear Technology and Engineering Center Operable Unit 3-13*, DOE/ID-10660, Rev. 0, U.S. Department of Energy Idaho Operations Office, October 1999.

DOE-ID, 2002, *Annual INTEC Groundwater Monitoring Report for Group 5 - Snake River Plain Aquifer (2001)*, DOE/ID-10930, Rev. 0, U.S. Department of Energy Idaho Operations Office, February 2002.

DOE-ID, 2003a, *Phase I Monitoring Well and Tracer Study Report for* OU *3-13, Group 4, Perched Water*, DOE/ID-10967, Rev. 2, U.S. Department of Energy Idaho Operations Office, March 2003. [Note: Revision 2 is Offical Use Only; Revision 1 is publicly avaiable.]

DOE-ID, 2003b, *INTEC Water System Engineering Study*, DOE/ID-11115, Rev. 0, U. S. Department of Energy Idaho Operations Office, December 2003.

DOE-ID, 2003c, *Performance Assessment for the INEEL CERCLA Disposal Facility Landfill,* DOE/ID-10978, Rev. 0, U.S. Department of Energy Idaho Operations Office, August 2003.

DOE-ID, 2003d, *Composite Analysis for the INEEL CERCLA Disposal Facility Landfill,* DOE/ID-10979, Rev. 0, U.S. Department of Energy Idaho Operations Office, August 2003.

DOE-ID, 2004a, *Operable Unit 3-14 Tank Farm Soil and Groundwater Remedial Investigation/Feasibility Study Work Plan*, DOE/ID-10676, Rev 1, U.S. Department of Energy Idaho Operations Office, June 2004.

DOE-ID, 2004b, *Vicinity Discharges Elimination Work Plan for the HWMA/RCAR Post-Closure Permit for the INTEC Waste Calcining Facility at the INEEL*, DOE/NE-ID-11138, Rev. 0, U.S. Department of Energy Idaho Operations Office, April 2004.

DOE-ID, 2004c, *Monitoring Report/Decision Summary for Operable Unit 3-13, Group 5, Snake River Plain Aquifer*, DOE/ID-11098, Rev. 1, U.S. Department of Energy Idaho Operations Office, December 2004.

DOE-ID, 2004d, *Operable Unit 3-13, Group 3, Other Surface Soils Remediation Sets 1-3 (Phase 1) Remedial Design/Remedial Action Work Plan*, DOE/ID-11089, Rev. 0, U.S. Department of Energy Idaho Operations Office, February 2004.

DOE-ID, 2005a, *Response to the First Five-Year Review Report for the Test Reactor Area, Operable Unit 2-13, at the Idaho National Engineering and Environmental Laboratory*, DOE/NE-ID-11189, U.S. Department of Energy Idaho Operations Office, May 2005.

DOE-ID, 2005b, *Waste Area Group 10, Operable Unit 10-08, Remedial Investigation/Feasibility Study Annual Status Report for Fiscal Year 2004*, DOE/NE-ID-11198, U.S. Department of Energy Idaho Operations Office, March 2005.

DOE/ID, 2006, *Annual INTEC Water Monitoring Report for Group 4—Perched Water (2005)*, DOE/ID-11259, U.S. Department of Energy Idaho Operations Office, Revision 0, January 2006.

Cecil, L. D., J. R. Pittman, T. M. Beasley, R. L. Michel, P. W. Kubik, P. Sharma, U. Fehn, and H. Gove, 1992, "Water Infiltration Rates in the Unsaturated Zone at the Idaho National Engineering Laboratory Estimated from Chlorine-36 and Tritium Profiles, and Neutron Logging," Y. K. Kharaka and A. S. Meest, eds., *Proceedings of the 7th International Symposium on Water-Rock Interaction - WRI-7, Park City, Utah.*

EDF-5758, 2005, "Geochemical Study For Perched Water Source Identification At INTEC," Rev. 0, Idaho National Laboratory, Idaho Cleanup Project, May 2005.

EDF-ER-275, 2005, "Fate and Transport Modeling Results and Summary Report," Rev. 4, Idaho National Engineering and Environmental Laboratory, Idaho Completion Project, January 2005.

EPA, 1988, "Limiting Values of Radionuclide Intake And Air Concentration and Dose Conversion Factors For Inhalation, Submersion, And Ingestion," Federal Guidance Report No. 11, EPA 520/1-88-020, U.S. Environmental Protection Agency, September 1988.

Frederick, D. B. and G. S. Johnson, 1996, *Estimation of Hydraulic Properties and Development of a Layered Conceptual Model for the Snake River Plain Aquifer at the Idaho National Engineering Laboratory, Idaho*, State of Idaho INEL Oversight Program, Idaho Water Resources Research Institute, February 1996.

Gee, G. W., D. G. Felmy, J. C. Ritter, M. D. Campbell, J. L. Downs, M. J. Fayer, R. R. Kirkham, and S. O. Link, 1993, *Field Lysimeter Test Facility Status Report IV: FY 1993*, PNL-8911 UC-902, Pacific Northwest Laboratory, 1993.

Golder Associates, Inc, 1992, *Report for the Idaho Chemical Processing Plant Drilling and Sampling Program at Land Disposal Unit CPP-37 (DRAFT)*, Prepared for EG&G Idaho, Inc./Westinghouse Idaho Nuclear Company, under Contract No. C90 132739, 903-1161, March 1992.

Honkus, R. J., 1982, *ICPP CY-1981 Effluent Monitoring Report*, ENICO-1115, Exxon Nuclear Idaho, Inc., May 1982.

ICP, 2004, *Evaluation of Tc-99 in Groundwater at INTEC: Summary of Phase 1 Results*, ICP/EXT-04-00244, Rev. 0, Idaho National Engineering and Enivronmental Laboratory, Idaho Completion Project, September 2004.

INEEL, 2003a, *Analysis of Baseline Data from ICDF Detection Monitoring Wells*, INEEL/EXT-03-00251, Rev. 0, Idaho National Engineering and Environmental Laboratory, August 2003.

INEEL, 2003b, *Comprehensive Facility and Land Use Plan*, http://cflup.inel.gov/, Idaho National Engineering and Environmental Laboratory, Web page created 2003, Web page visited March 16, 2005.

INEL, 1995a, *Report of 1993/1994 Tank Farm Drilling and Sampling Investigation at the Idaho Chemical Processing Plant*, INEL-95/0064, Idaho National Engineering Laboratory, February 1995.

INEL, 1995b, *Waste Area Group 3 Comprehensive Remedial Investigation/Feasibility Study Work Plan (FINAL)*, INEL-95/0056, Vol.1, Idaho National Engineering Laboratory, August 1995.

Kehow, A. E., 2001, *Applied Chemical Hydrogeology*, Upper Saddle River, New Jersey: Prentice-Hall, Inc..

Knutson, C. F., K. A. McCormick, R. P. Smith, W. R. Hackett, J. P. O'Brien, and J. C. Crocker, 1990, *FY 89 Report RWMC Vadose Zone Basalt Characterization*, EGG-WM-8949, EG&G Idaho, Inc., Idaho National Engineering Laboratory, July 1990.

Magnuson, S. O., 1995, *Inverse Modeling for Field-Scale Hydrologic and Transport Parameters of Fractured Basalt*, INEL-95/0637, Idaho National Engineering Laboratory, December 1995.

Magnuson, S. O. and A. J. Sondrup, 1998, *Development, Calibration, and Predictive Results of a Simulator for Subsurface Pathway Fate and Transport of Aqueous- and Gaseous-Phase Contaminants in the Subsurface Disposal Area at the Idaho National Engineering and Environmental Laboratory*, INEEL/EXT-97-00609, Idaho National Engineering and Environmental Laboratory, July 1998.

Martian, P., 1995, *UNSAT-H Infiltration Model Calibration at the Subsurface Disposal Area, Idaho National Engineering Laboratory*, INEL-95/0596, Idaho National Engineering Laboratory, October 1995.

Martian, P., 1999, *Numerical Modeling Support of the Natural Attenuation Field Evaluation for Trichloethene at the Test Area North, Operable Unit 1-07B, Idaho National Engineering and Environmental Laboratory*, INEEL/EXT-97-01284, Rev. 1, Idaho National Engineering and Environmental Laboratory, January 1999.

NCRP, 1996, *Screening Models for Release of Radionuclides to Atmosphere, Surface Water, and Ground*, NCRP Report No. 123 I&II, National Council on Radiation Protection, January 1996.

Orr, B. R., L. D. Cecil, and L. L. Knoble, 1991, "Background Concentrations of Selected Radionuclides, Organic Compounds, and Chemical Constituents in Ground Water in the Vicinity of the Idaho National Engineering Laboratory," U. S. Geological Survey-Water Resources Investigations Report 91-4015.

Parker, J. C., R. J. Lenhard, and T. Kuppusamy, 1987, "A Parametric Model for Constitutive Properties Governing Multiphase Flow in Porous Media," *Water Resources Research*, Vol. 23, No. 4, pp. 618-624.

Perry, R. H., D. W. Green, and J. O. Maloney, 1984, *Perry's Chemical Engineers' Handbook, Sixth Edition*, New York: McGraw Hill Book Company.

Roback, R. C., T. M. Johnson, T. L. McLing, M. T. Murrell, S. Luo, and T. L. Ku, 2001, "Uranium Isotopic Evidence for Groundwater Evolution and Flow Patterns in the Eastern Snake River Plain Aquifer," *Idaho Geologic Society America Bulletin*, 113, pp. 1133-1141.

Robertson, J. B., R. Schoen, and J. T. Barraclough, 1974, "The Influence of Liquid Waste Disposal on the Geochemistry of Water at the National Reactor Testing Station, Idaho: 1952-1970," IDO-22053, TID-4500, U.S. Geological Survey Open File Report, February 1974.

Rood, A. S., 1999, *GWSCREEN: A Semi-Analytical Model for Assessment of the Groundwater Pathway from Surface or Buried Contamination*, INEEL/EXT-98-00750 (Revised July 17, 2002), Idaho National Engineering and Environmental Laboratory, February 1999.

Sheppard, M. J., and D. H. Thibault, 1990, "Default Soil Solid/Liquid Partition Coefficients Kd's for Four Major Soil Types: A Compendium," *Health Physics* 59(4), pp. 471-482, 1990.

Shook, G. M., 1995, *Development of an Environmental Simulator from Existing Petroleum Technology*, INEL-94/0283, Idaho National Engineering Laboratory.

Shook, G. M., J. H. Forsmann, M. E. Velasquez, and S. O. Magnuson, 2003, "Improving Numerical Model Efficiency of an Existing, In-House Simulation Model," *Laboratory-Directed Research and Development, FY-2003 Annual Report*, INEEL/EXT-04-01772, Idaho National Engineering and Environmental Laboratory, pp. 197-199.

Smith, R. P., 2002, *Aquifer Thickness Assessment for Use in WAG 10*, OU *10-08 Groundwater Modeling Activities*, INEEL/INT-01-01458, Rev. 0, Idaho National Engineering and Environmental Laboratory, February 2002.

USGS, 2004, *NWISWeb Data for the Nation*, http://waterdata.usgs.gov/nwis, U.S. Geological Survey, Web page visited December 15, 2005.

Vinsome, P. K. W. and G. M. Shook, 1993, "Multi-Purpose Simulation," *Journal of Petroleum Science and Engineering*, Vol. 9, pp. 29-38, Elsevier Science Publishers B. V., Amsterdam.

Wood, T. R., 1989, *Test Area North Pumping Tests 1953-1987*, EGG-ER-8438, EG& G Idaho, Idaho National Engineering Laboratory, January 1989.

Van Genuchten, M. Th., 1980, "A Closed-Form Equation for Predicting the Hydraulic Conductivity of Unsaturated Soils," *Soil Science Society of America Journal*, 44, pp. 892-898.